Electronic Supplementary Material (ESI) for RSC Advances.

Supporting information

An efficient multichannel probe to detect anions in different medium and its real application in human blood plasma

Syed S. Razi, Rashid Ali, Priyanka Srivastava, Mohammad Shahid and Arvind Misra*

Department of Chemistry, Faculty of Science, Banaras Hindu University, Varanasi – 221 005. INDIA.

Corresponding author: arvindmisra2003@yahoo.com; amisra@bhu.ac.in
Tel: +91-542-6702503; Fax: +91-0542-2368127, 2368175.

Figure S1: ^{1}H NMR spectrum of **2** in $CDCl_3$.

Figure S2: ^{1}H NMR spectrum of **3** in $CDCl_3$.

Figure S3: D_2O exchange NMR spectrum of **3** in $CDCl_3$.

Figure S4: FTIR spectrum of **3**.

Figure S5: ^{13}C NMR spectrum of **3** in $CDCl_3$.

Figure S6: Mass spectrum (ESI-MS) of **3**.

Figure S7: ^{1}H NMR spectrum of **4** in $CDCl_3$.

Figure S8: FTIR spectrum of **4**.

Figure S9: ^{13}C NMR spectrum of **4** in $CDCl_3$.

Figure S10: Solvatochromic behavior of **3** (10 μM) in (a) absorption, (b) emission spectra and table of absorption and emission data and (c) Absorption spectra of **3** (10 μM) with TBAOH (10 equiv) in ACN. Inset: change in color of **3** after addition of TBAOH.

Figure S11: (a) Absorption titration spectra of **3** (10 μM) with AcO^- (0-5 equiv). Inset: Job's plot and (b) Benesi-Hildebrand plot.

Figure S12: Change in absorption spectra of **4** (10 μM) with different anions (10 equiv) as F^-, Cl^-, Br^-, I^-, S^{2-}, N_3^-, SCN^-, AcO^-, CN^-, $H_2PO_4^-$ (as their tetrabutylammonium salts) in MeCN. Inset: Colorimetric response of **3** (A) (10 μM) with different anions (10 equiv) (B) (10^{-2} M) with different anions (10^{-2} M) as F^-, Cl^-, Br^-, I^-, S^{2-}, N_3^-, SCN^-, AcO^-, CN^-, $H_2PO_4^-$ and HS^- (as their sodium salts) in aqueous medium.

Figure S13: Absorption and emission spectra of **3** (a, b) and **4** (c, d) at different pHs.

Figure S14: Interference studies illustrating change in absorption and emission spectra upon addition of different anions (200 equiv) to a solution of **3+CN$^-$** and **4+CN$^-$** (10 μM) in aqueous medium. Images: Change in color of probes **3** and **4** upon interaction with different anions in aqueous medium (UV = 365 nm).

Figure S15: ^{1}H NMR titration spectrum of **3** with 0.1 equiv of F^- in $CDCl_3$.

Figure S16: ^{1}H NMR titration spectrum of **3** with 0.2 equiv of F^- in $CDCl_3$.

Figure S17: ^{1}H NMR titration spectrum of **3** with 0.3 equiv of F^- in $CDCl_3$.

Figure S18: ^{1}H NMR titration spectrum of **3** with 0.4 equiv of F^- in $CDCl_3$.

Figure S19: ^{1}H NMR titration spectrum of **3** with 0.6 equiv of F^- in $CDCl_3$.

Figure S20: ^{1}H NMR titration spectrum of **3** with 0.8 equiv of F^- in $CDCl_3$.

Figure S21: ^{1}H NMR titration spectrum of **3** with 1.2 equiv of F^- in $CDCl_3$.

Figure S22: Stacked ^{1}H NMR titration spectra of **3** upon addition of AcO^- (0, 0.1, 0.2, 0.3, and 0.4 equiv) in $CDCl_3$.

Figure S23: ^{1}H NMR titration spectrum of **3** with 0.1 equiv of AcO^- in $CDCl_3$.

Figure S24: ^{1}H NMR titration spectrum of **3** with 0.2 equiv of AcO^- in $CDCl_3$.

Figure S25: ^{1}H NMR titration spectrum of **3** with 0.3 equiv of AcO^- in $CDCl_3$.

Figure S26: ^{1}H NMR titration spectrum of **3** with 0.4 equiv of AcO^- in $CDCl_3$.

Figure S27: ^{13}CNMR spectrum of adduct, **3-CN**$^-$ in $CDCl_3$/DMSO-d_6.

Figure S28: ^{13}CNMR spectrum of adduct, **4-CN**$^-$.

Figure S29: FTIR spectrum of adduct, **3-CN**$^-$.

Figure S30: FTIR spectrum of adduct, **4-CN**$^-$.

Figure S31: Mass spectrum (ESI-MS) of **3-CN**.

Figure S32: ^{1}HNMR spectrum of adduct, **3-CN**$^-$.

Figure S33: ^{1}HNMR spectrum of adduct, **4-CN**$^-$. Inset: stacked ^{1}HNMR spectra of **4** and **4-CN**$^-$.

Figure S34: D_2O exchange ^{1}HNMR spectrum of adduct, **4-CN**$^-$.

Figure S35: (a) Calibration curve for **3,** (b) calibration sensitivity for CN^- in H_2O.

Figure S36: (a) Calibration curve for **3,** (b) and (c) calibration sensitivities for F^- and AcO^- in MeCN.

Figure S37: (a) Calibration curve for **3,** (b) calibration sensitivity for CN^- in human blood plasma.

Figure S38: Stacked ^{1}H NMR titration spectra of **3** upon addition of F^- (0, 0.2, 0.4 and 0.6, equiv) in DMSO-d_6.

Figure S39: ^{1}H NMR spectrum of **3** in DMSO-d_6.

Figure S40: ^{1}H NMR titration spectrum of **3** with 0.2 equiv of F^- in DMSO-d_6.

Figure S41: ^{1}H NMR titration spectrum of **3** with 0.4 equiv of F^- in DMSO-d_6.

Figure S42: ^{1}H NMR titration spectrum of **3** with 0.6 equiv of F^- in DMSO-d_6.

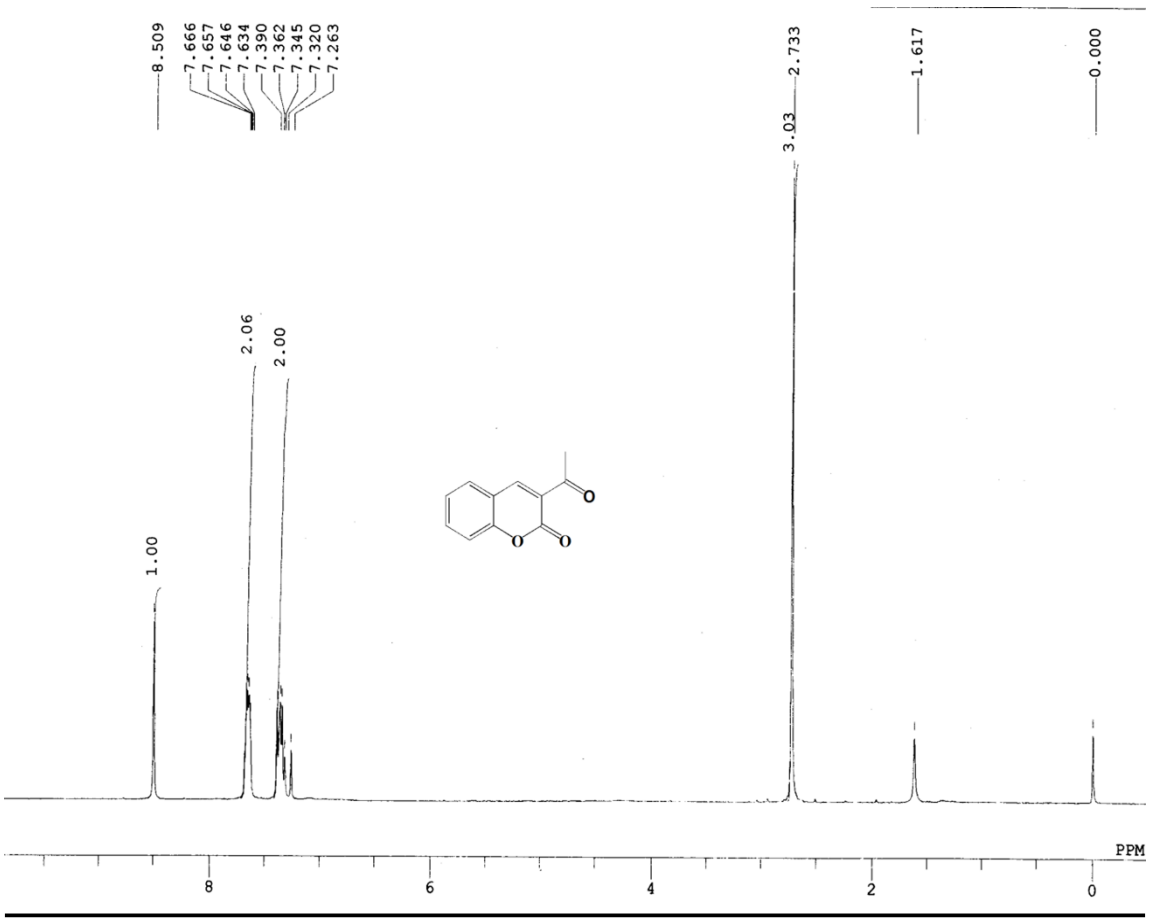

Figure S1: ^{1}H NMR spectrum of **2** in $CDCl_3$.

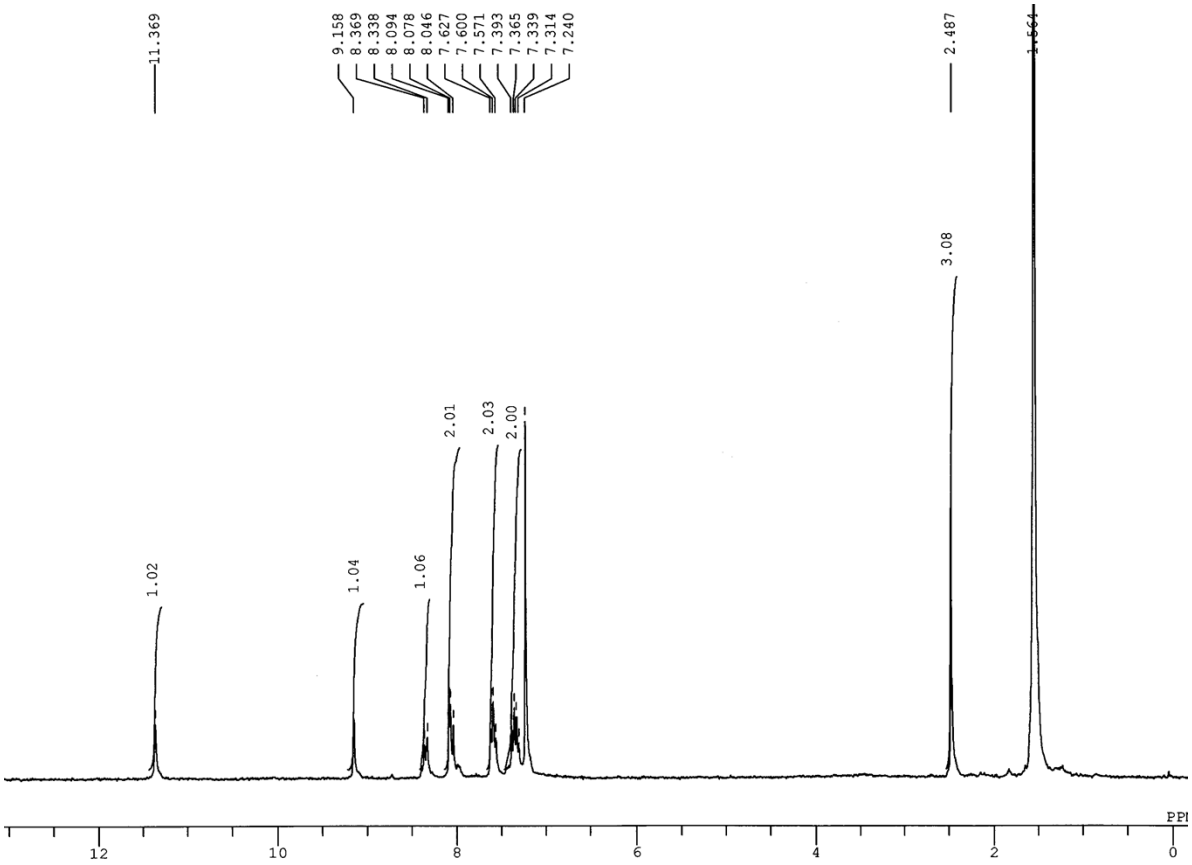

Figure S2: ^{1}H NMR spectrum of **3** in $CDCl_3$.

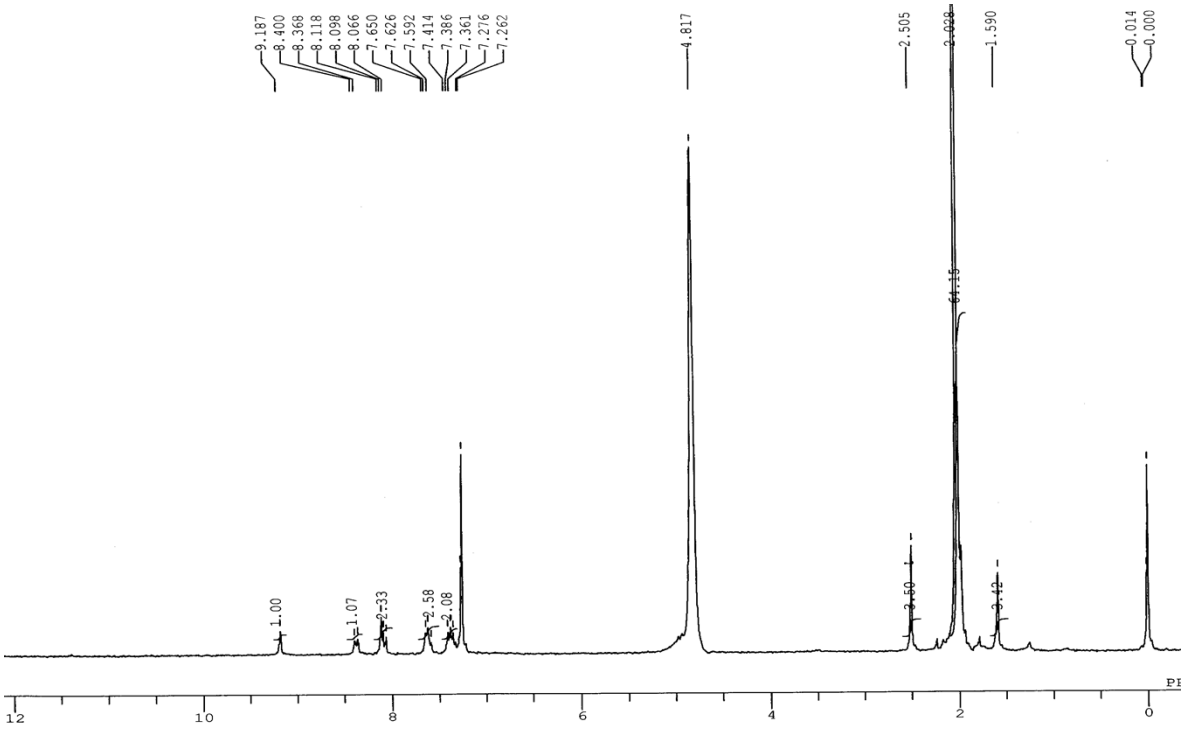

Figure S3: D_2O exchange NMR spectrum of **3** in $CDCl_3$.

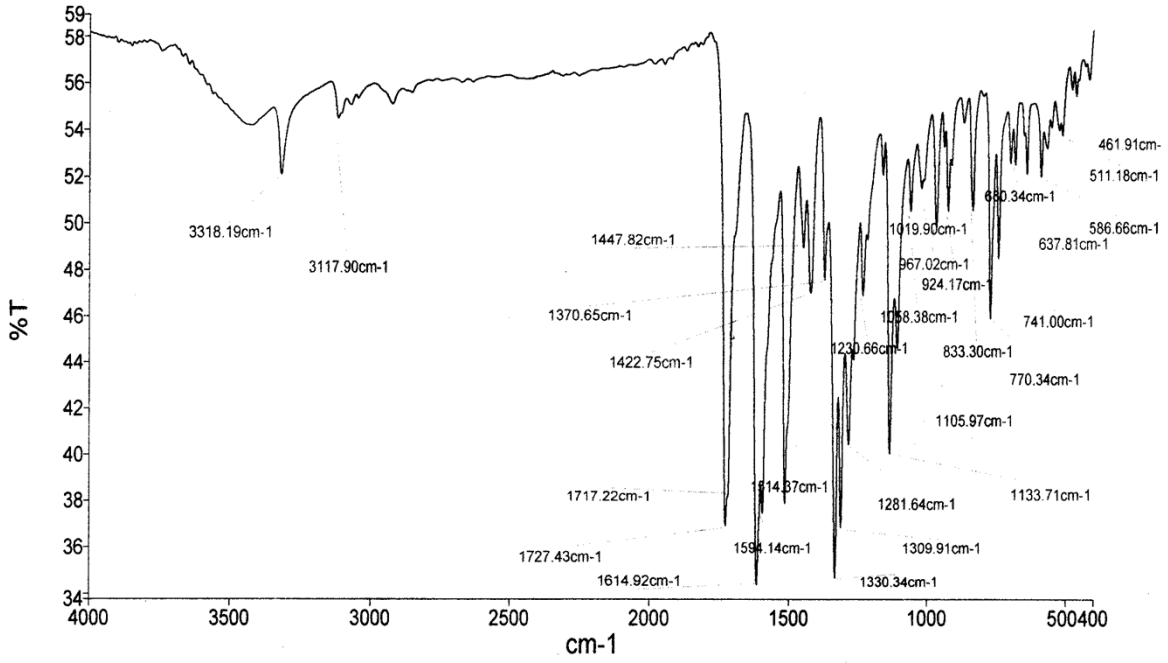

Figure S4: FTIR spectrum of **3**.

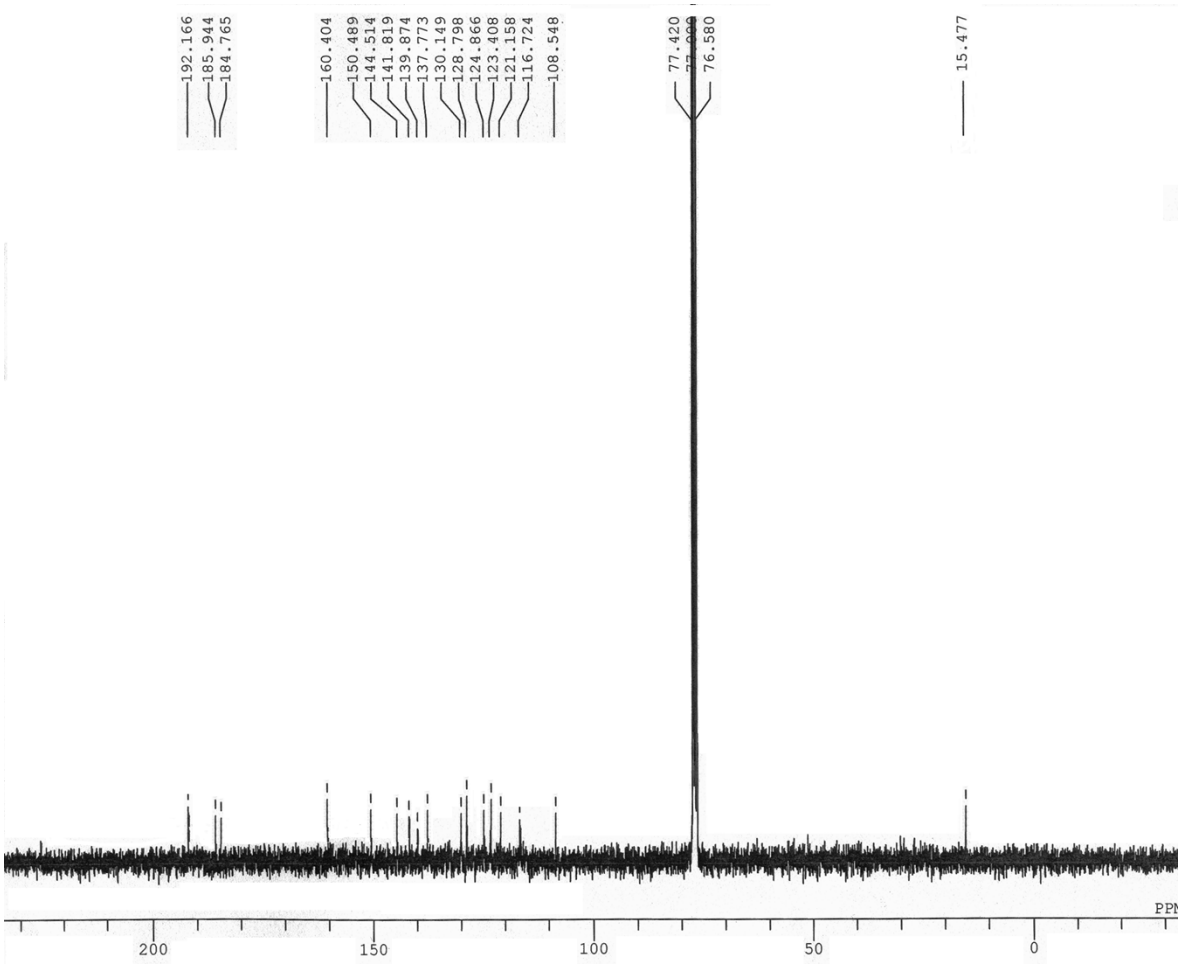

Figure S5: ^{13}C NMR spectrum of **3** in $CDCl_3$.

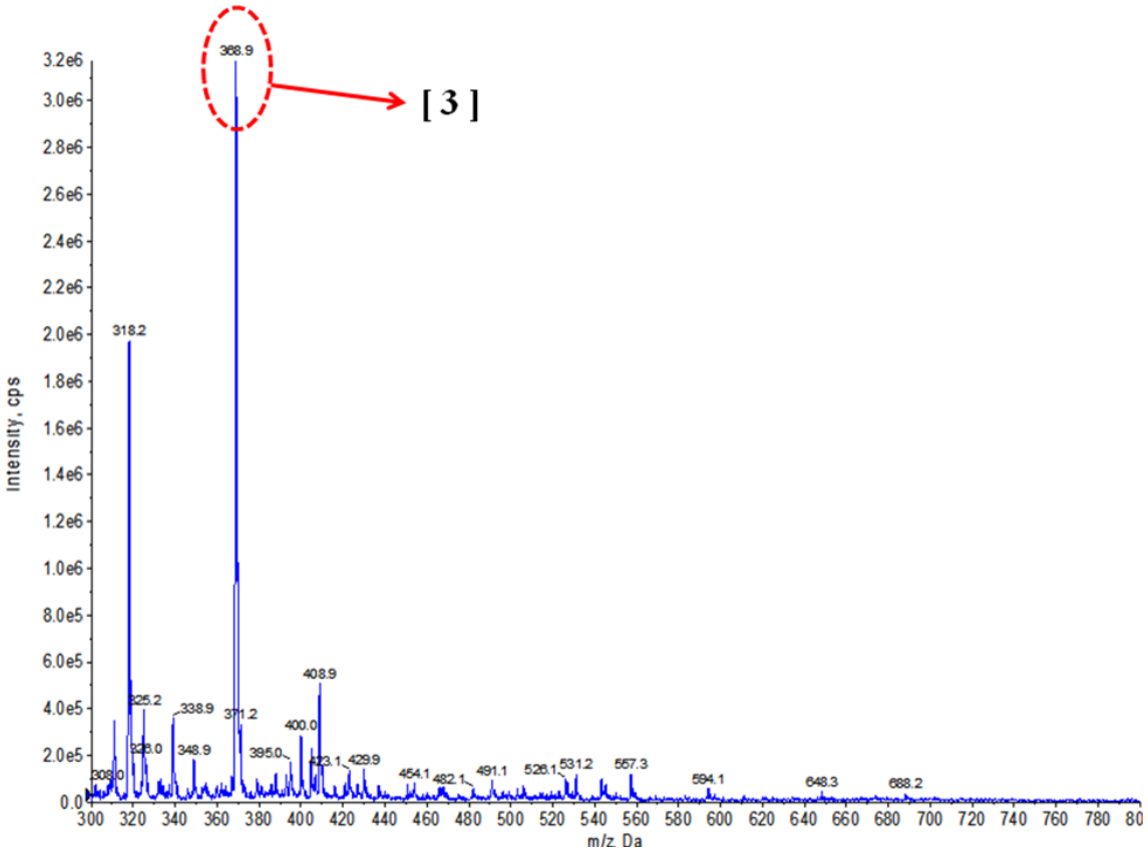

Figure S6: Mass spectrum (ESI-MS) of **3**.

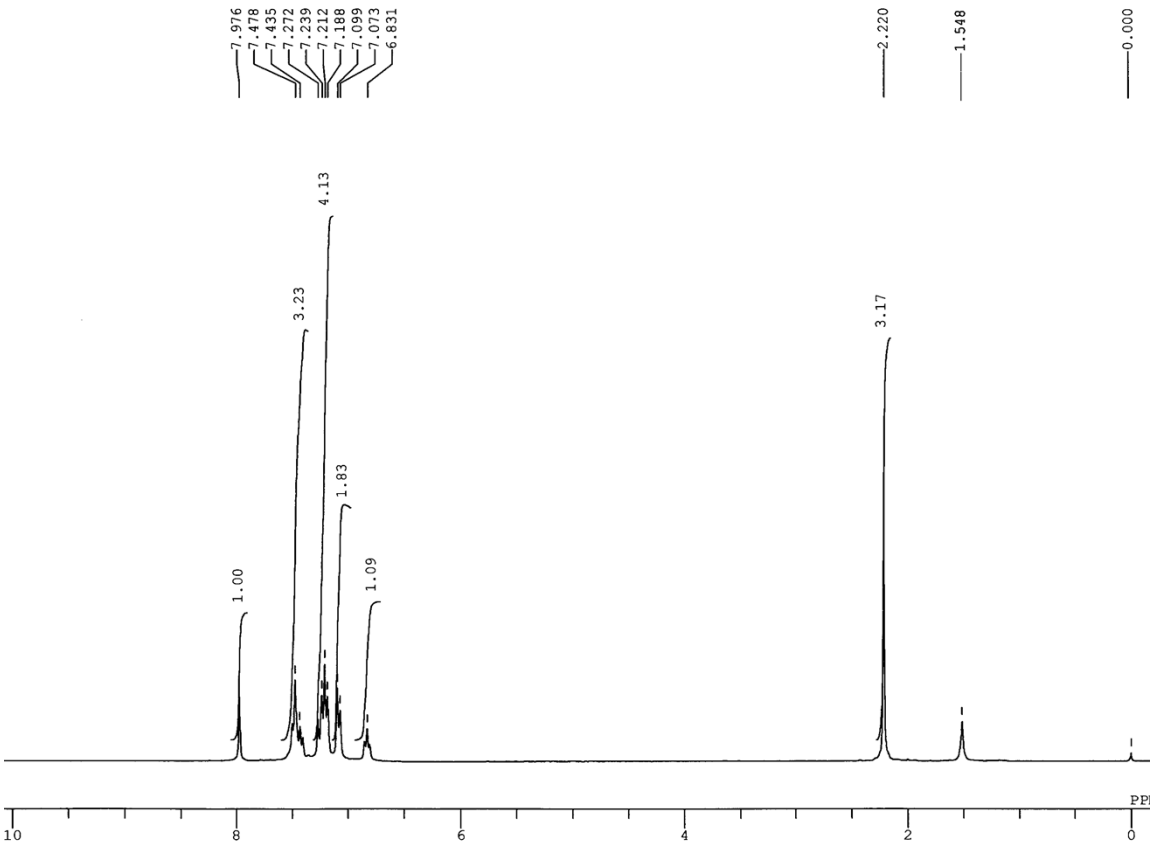

Figure S7: ^{1}H NMR spectrum of **4** in $CDCl_3$.

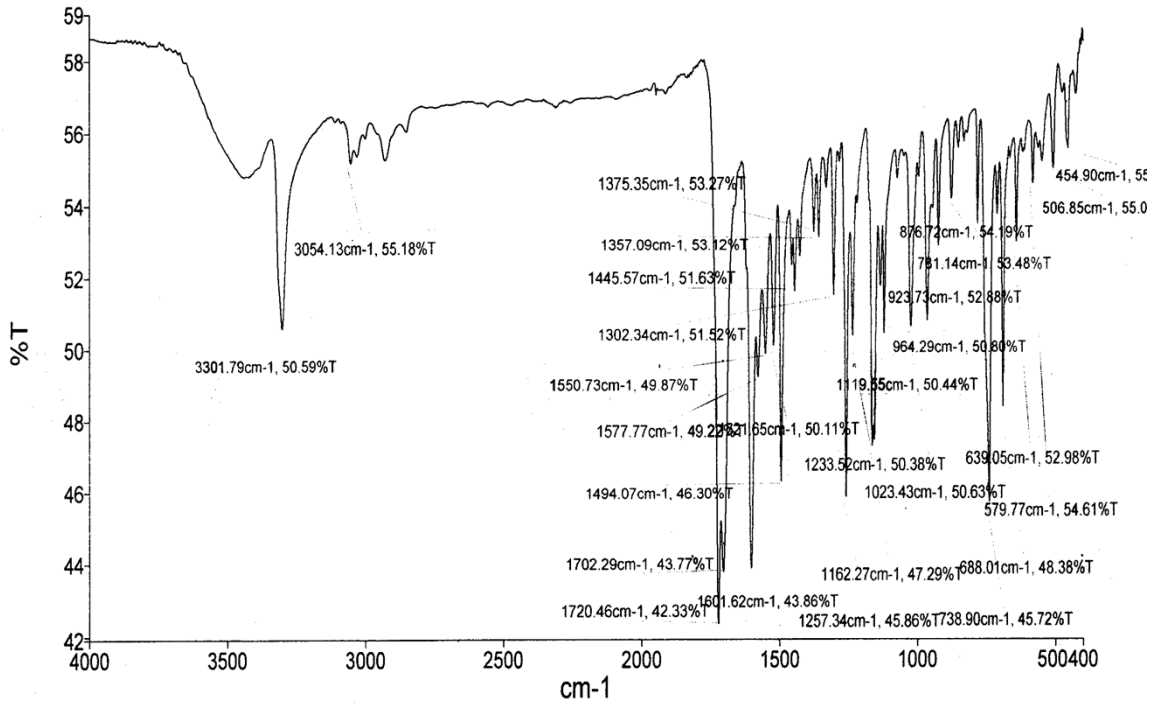

Figure S8: FTIR spectrum of **4**.

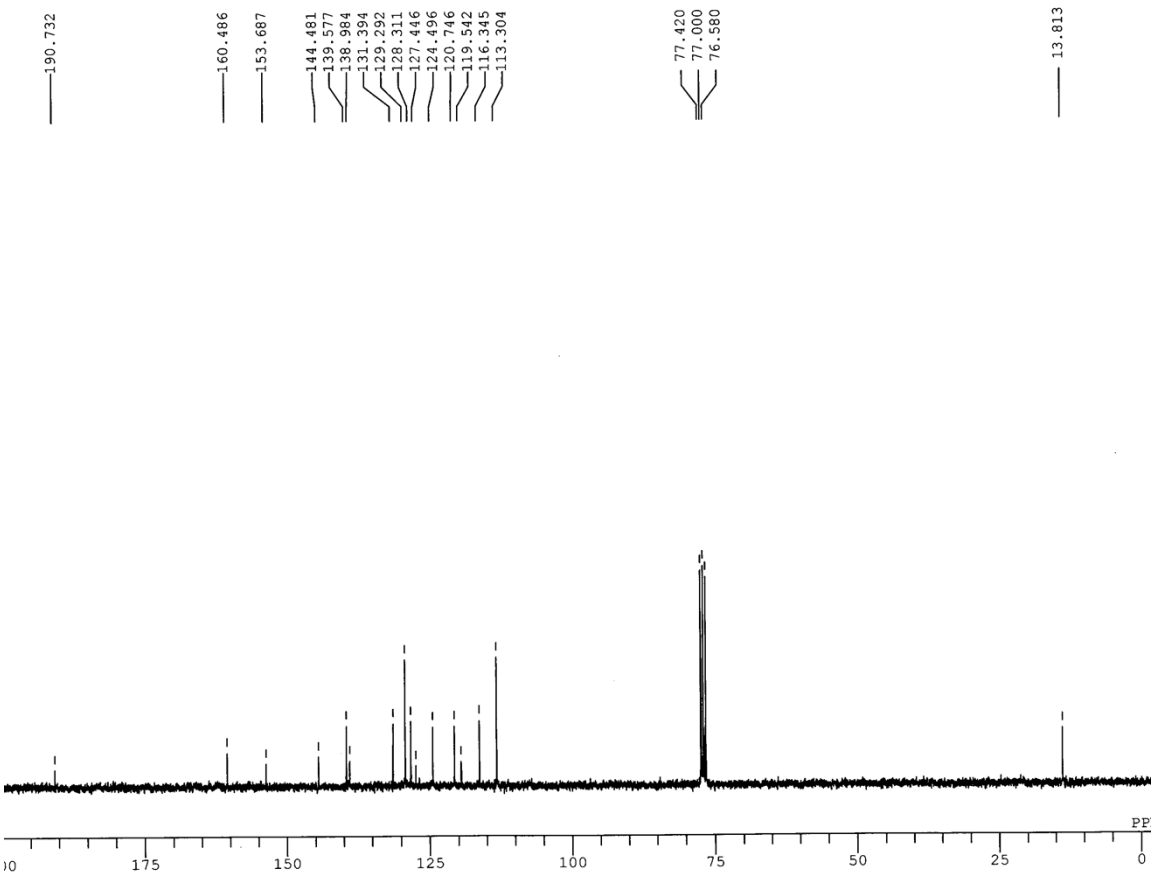

Figure S9: ^{13}C NMR spectrum of **4** in $CDCl_3$.

Table S1

Solvents	λ_{Abs} ***(in nm)*** ($\varepsilon = M^{-1} cm^{-1}$)	λ_{em} ***(in nm)***
ACN	378 (2.9 x 10^4)	435
DMSO	389 (2.86 x 10^4)	450
THF	379 (3.22 x 10^4)	438
MeOH	381 (3.0 x 10^4)	429
DCM	380 (2.82 x 10^4)	438
Benzene	382 (3.49 x 10^4)	435

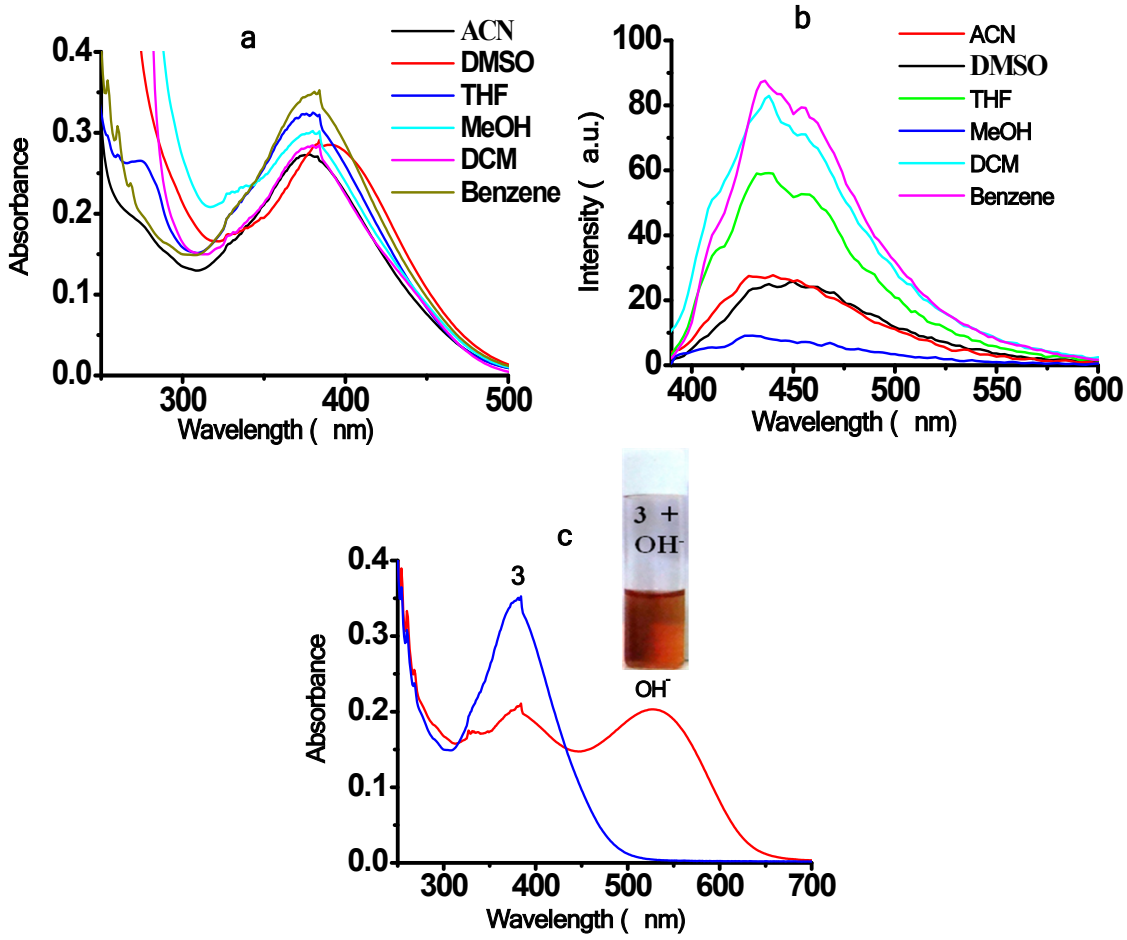

Figure S10: Solvatochromic behavior of **3** (10 μM) in (a) absorption, (b) emission spectra and table of absorption and emission data and (c) Absorption spectra of **3** (10 μM) with TBAOH (10 equiv) in ACN. Inset: change in color of **3** after addition of TBAOH.

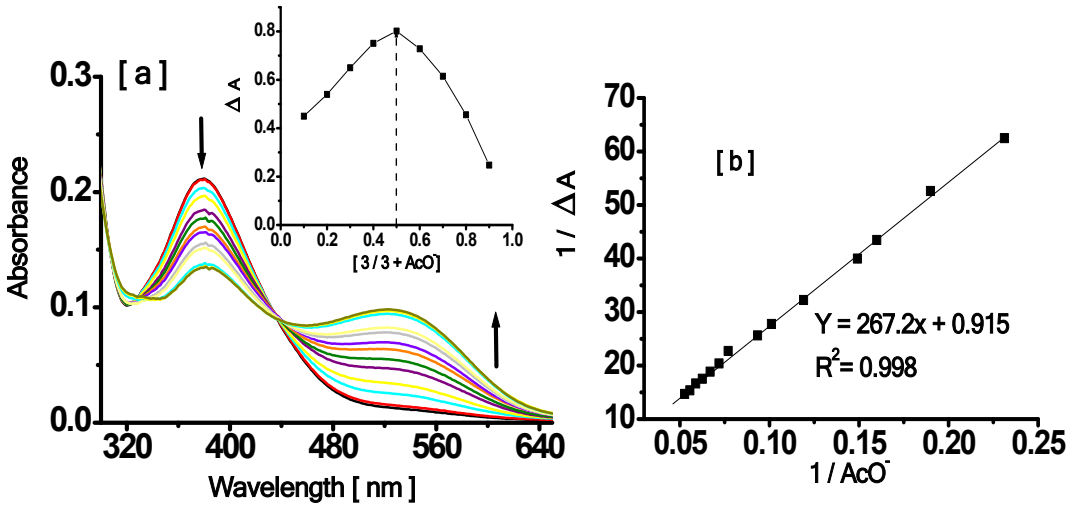

Figure S11: (a) Absorption titration spectra of **3** (10 μM) with AcO^- (0-5 equiv) ions. Inset: Job's plot and (b) Benesi-Hildebrand plot.

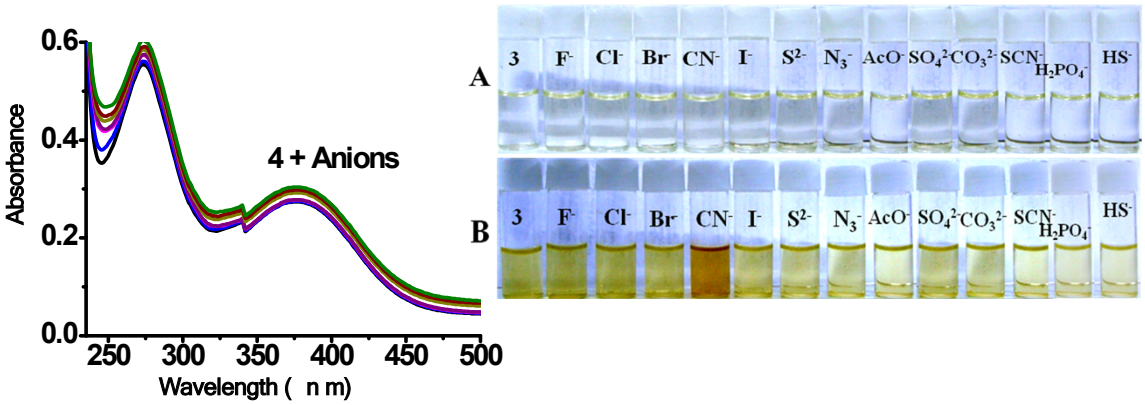

Figure S12: Change in absorption spectra of **4** (10 μM) with different anions (10 equiv) as F^-, Cl^-, Br^-, I^-, S^{2-}, N_3^-, SCN^-, AcO^-, CN^-, $H_2PO_4^-$ (as their tetrabutylammonium salts) in MeCN. Inset: Colorimetric response of **3** (A) (10 μM) with different anions (10 equiv) (B) (10 mM) with different anions (10 mM) as F^-, Cl^-, Br^-, I^-, S^{2-}, N_3^-, SCN^-, AcO^-, CN^-, $H_2PO_4^-$ and HS^- (as their sodium salts) in aqueous medium.

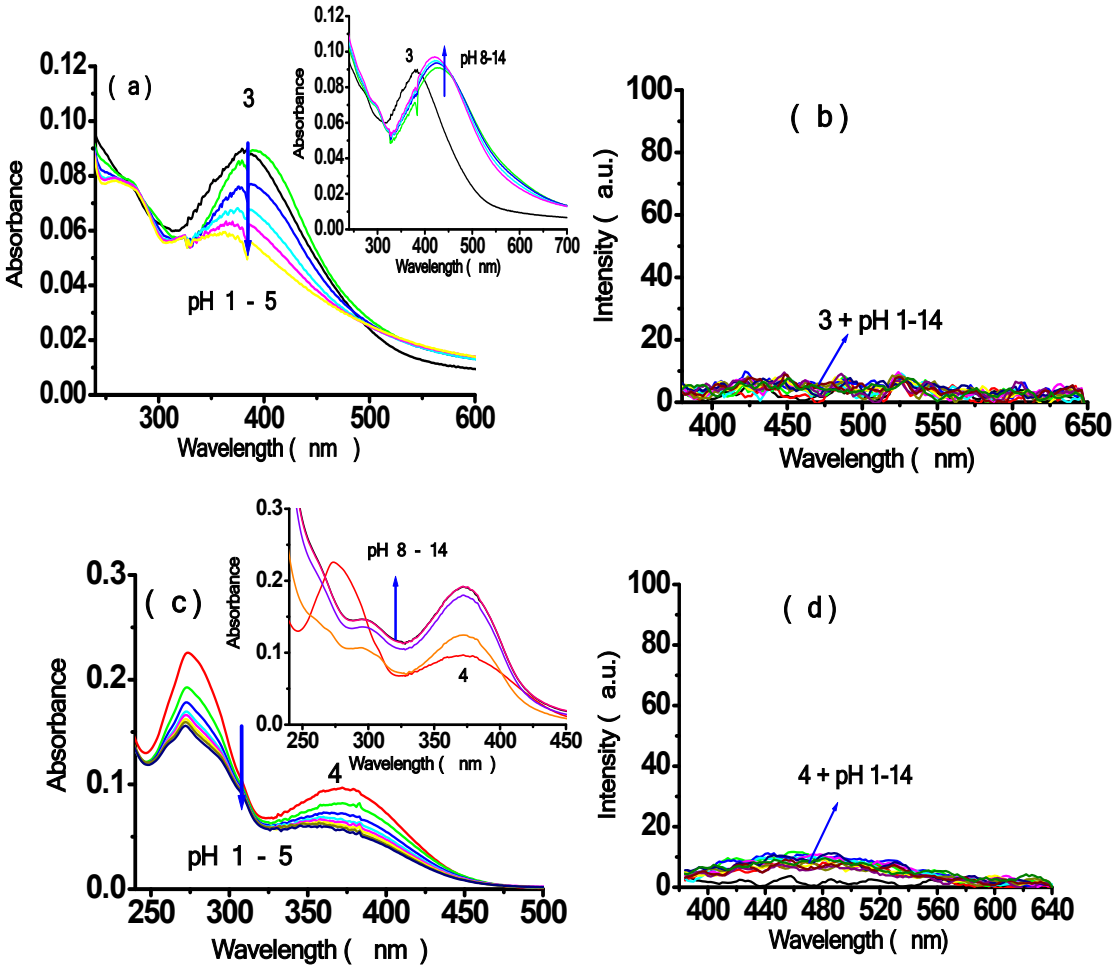

Figure S13: Absorption and emission spectra of **3** (a, b) and **4** (c, d) at different pHs.

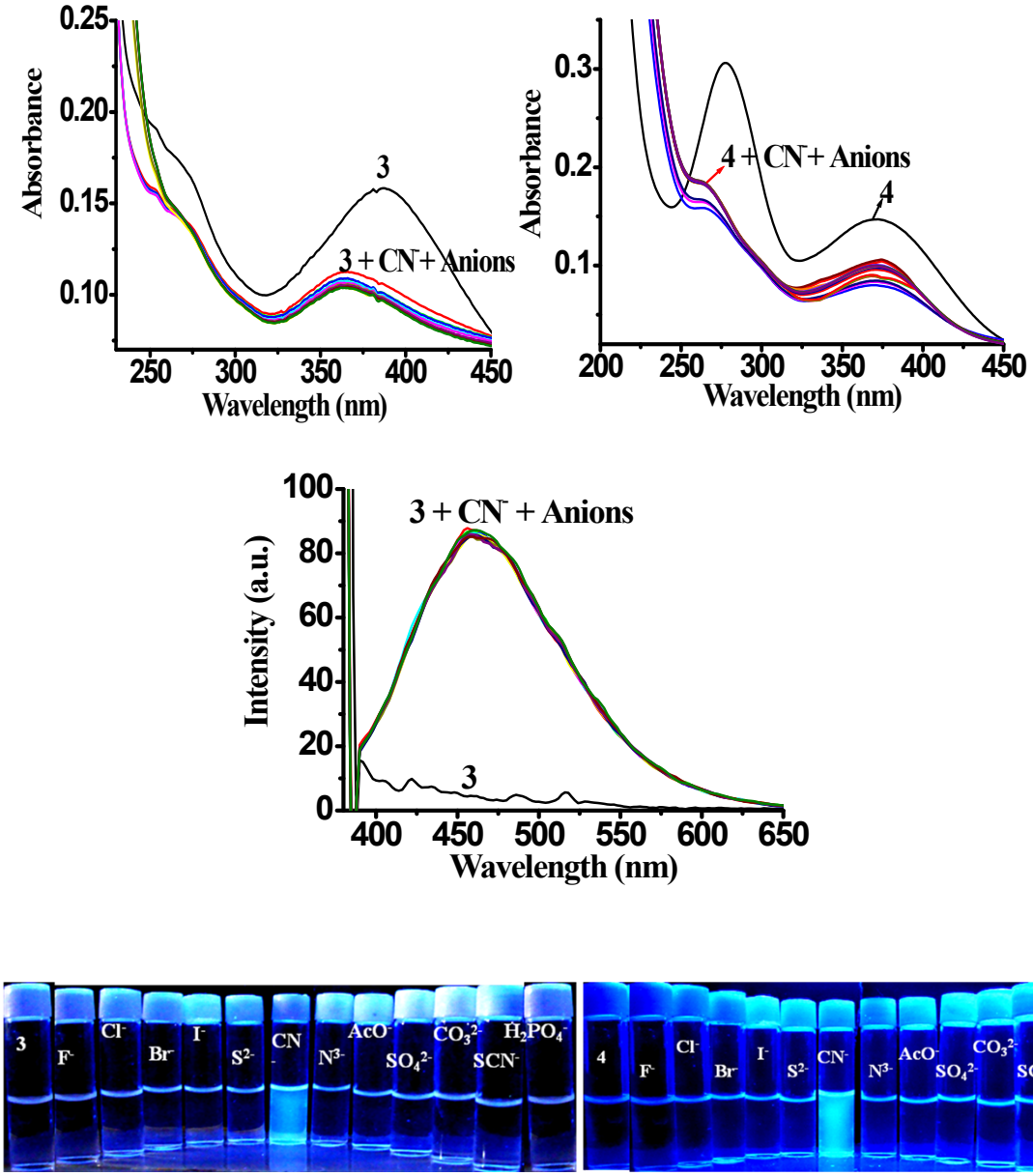

Figure S14: Interference studies illustrating change in absorption and emission spectra upon addition of different anions (200 equiv) to a solution of **3**+CN^- and **4**+CN^- (10 μM) in aqueous medium. Images: Change in color of probes **3** and **4** upon interaction with different anions in aqueous medium (UV = 365 nm).

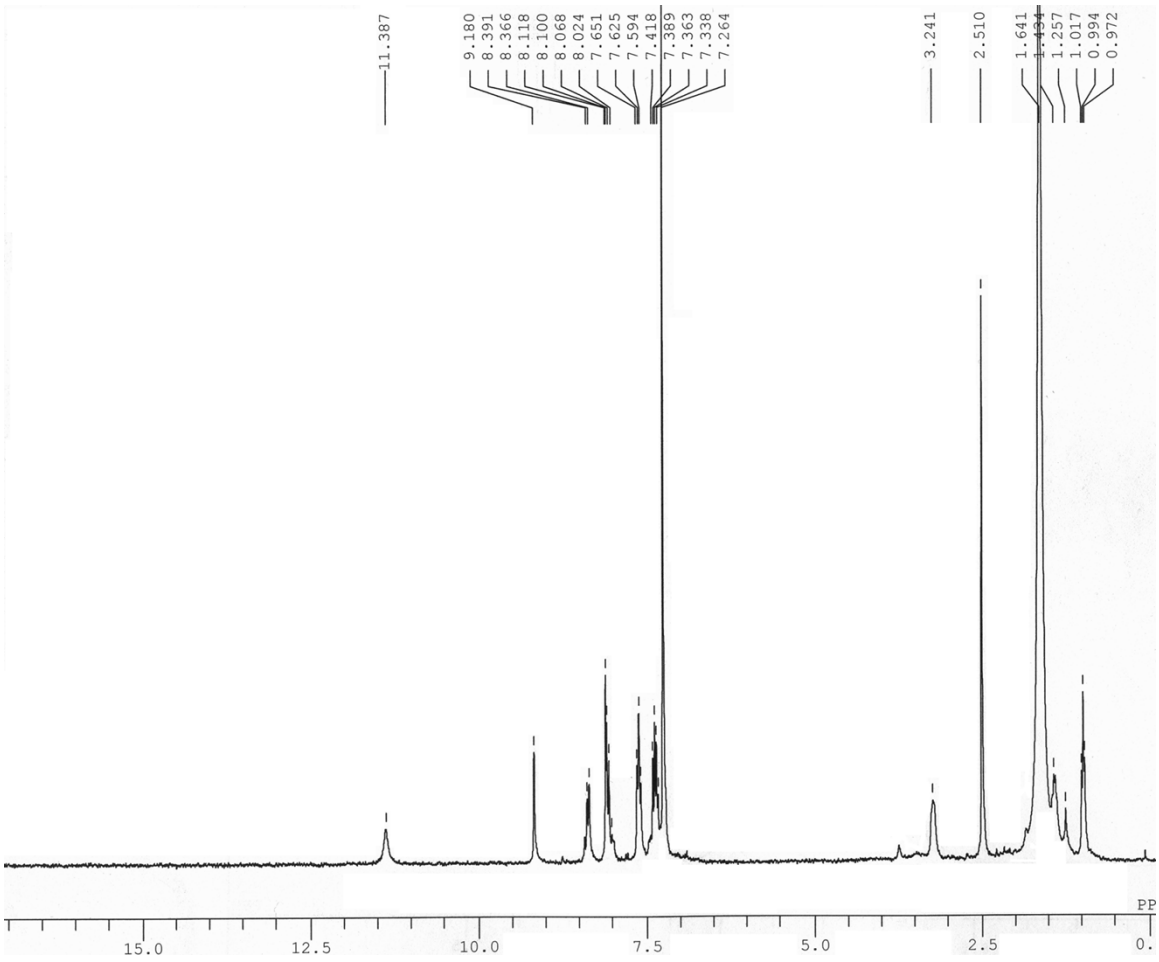

Figure S15: ^{1}H NMR titration spectrum of **3** with 0.1 equiv of F^- in $CDCl_3$.

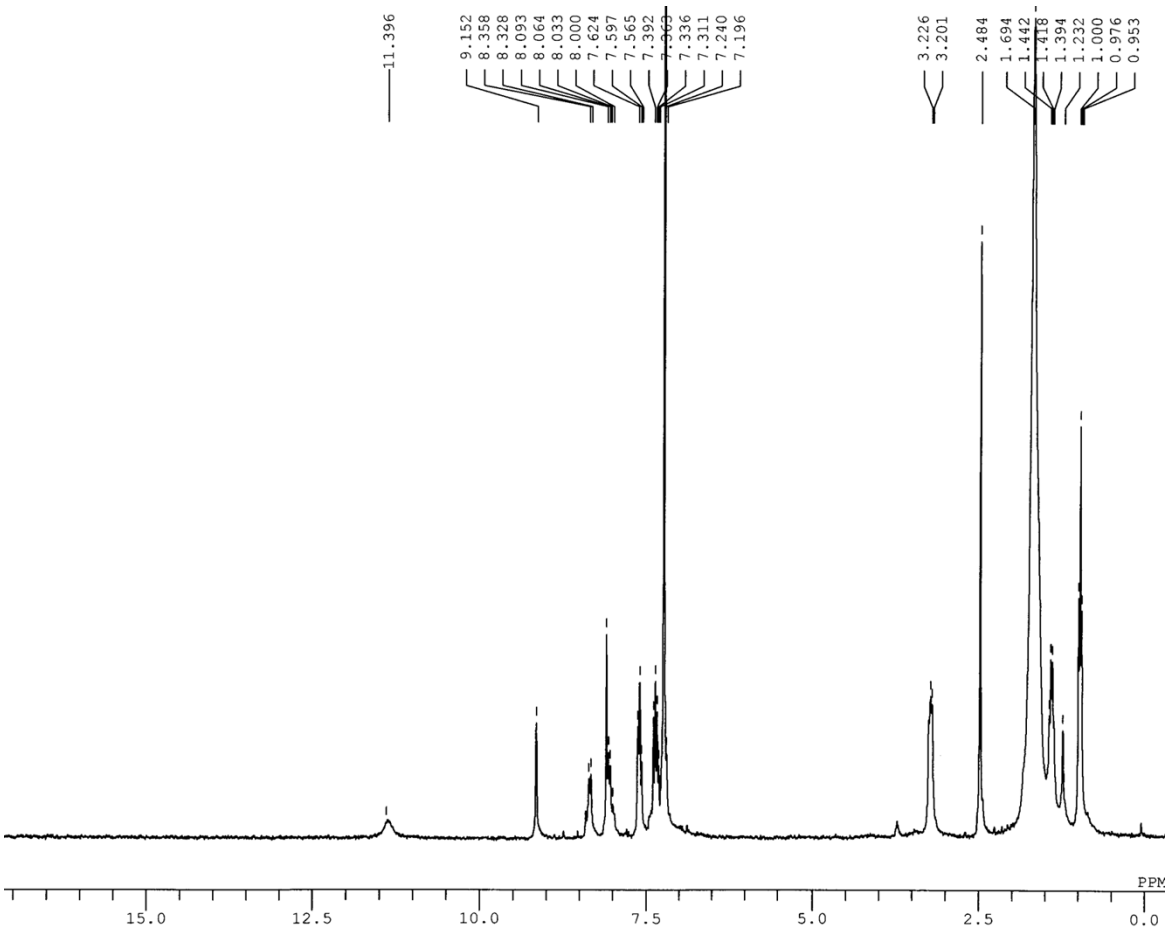

Figure S16: ^{1}H NMR titration spectrum of **3** with 0.2 equiv of F^- in $CDCl_3$.

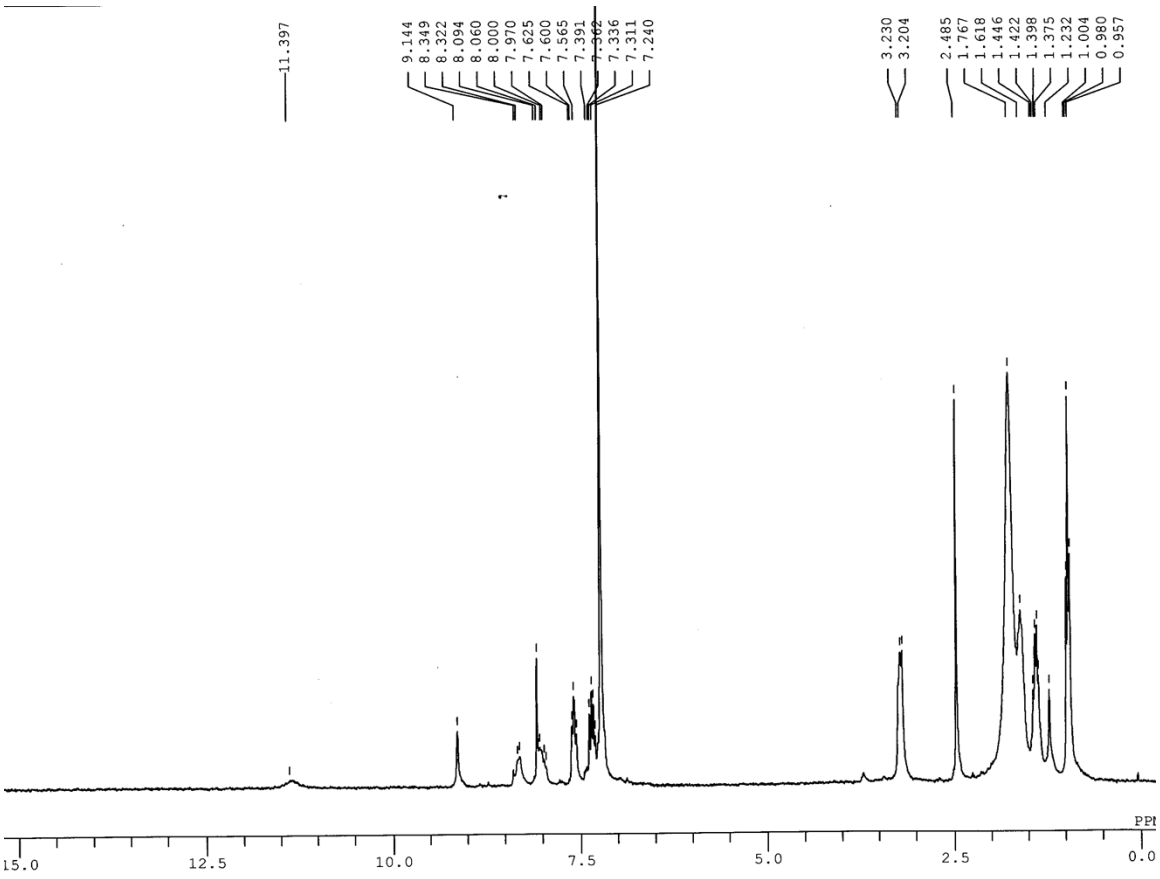

Figure S17: ^{1}H NMR titration spectrum of **3** with 0.3 equiv of F^- in $CDCl_3$.

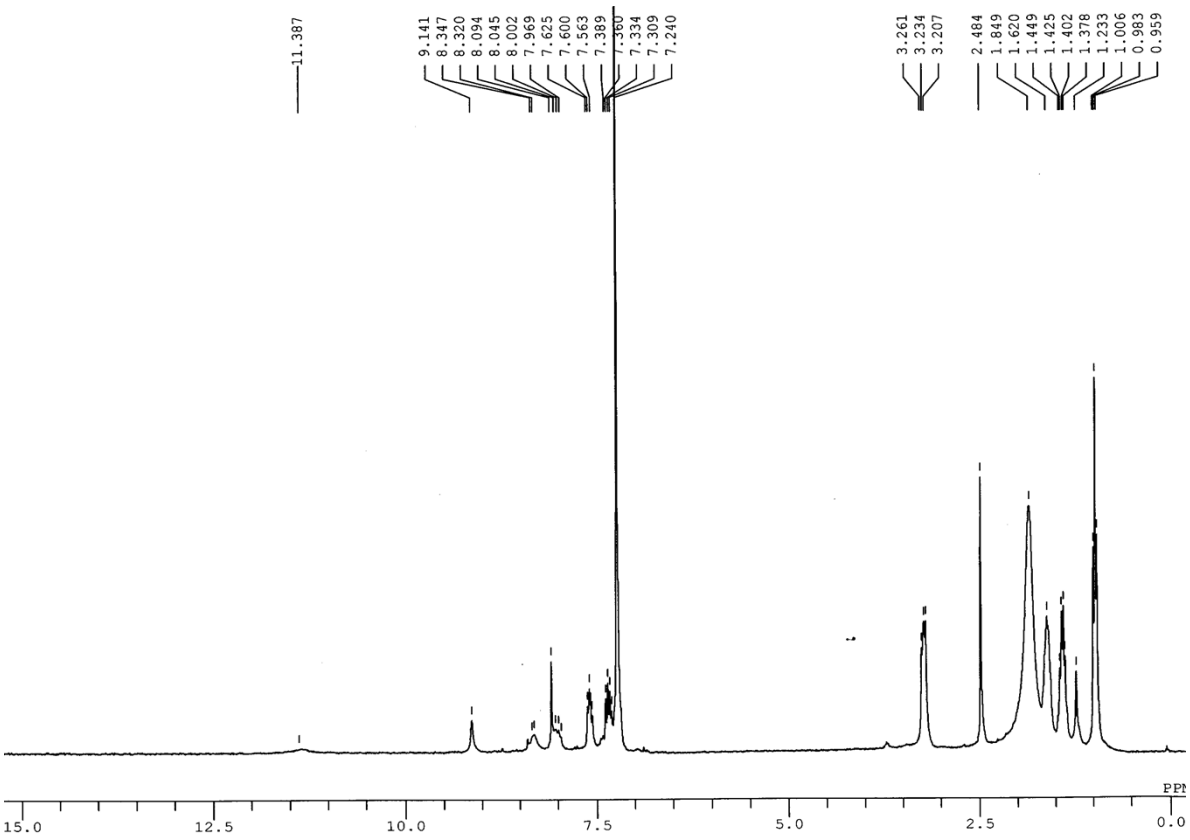

Figure S18: ^{1}H NMR titration spectrum of **3** with 0.4 equiv of F^- in $CDCl_3$.

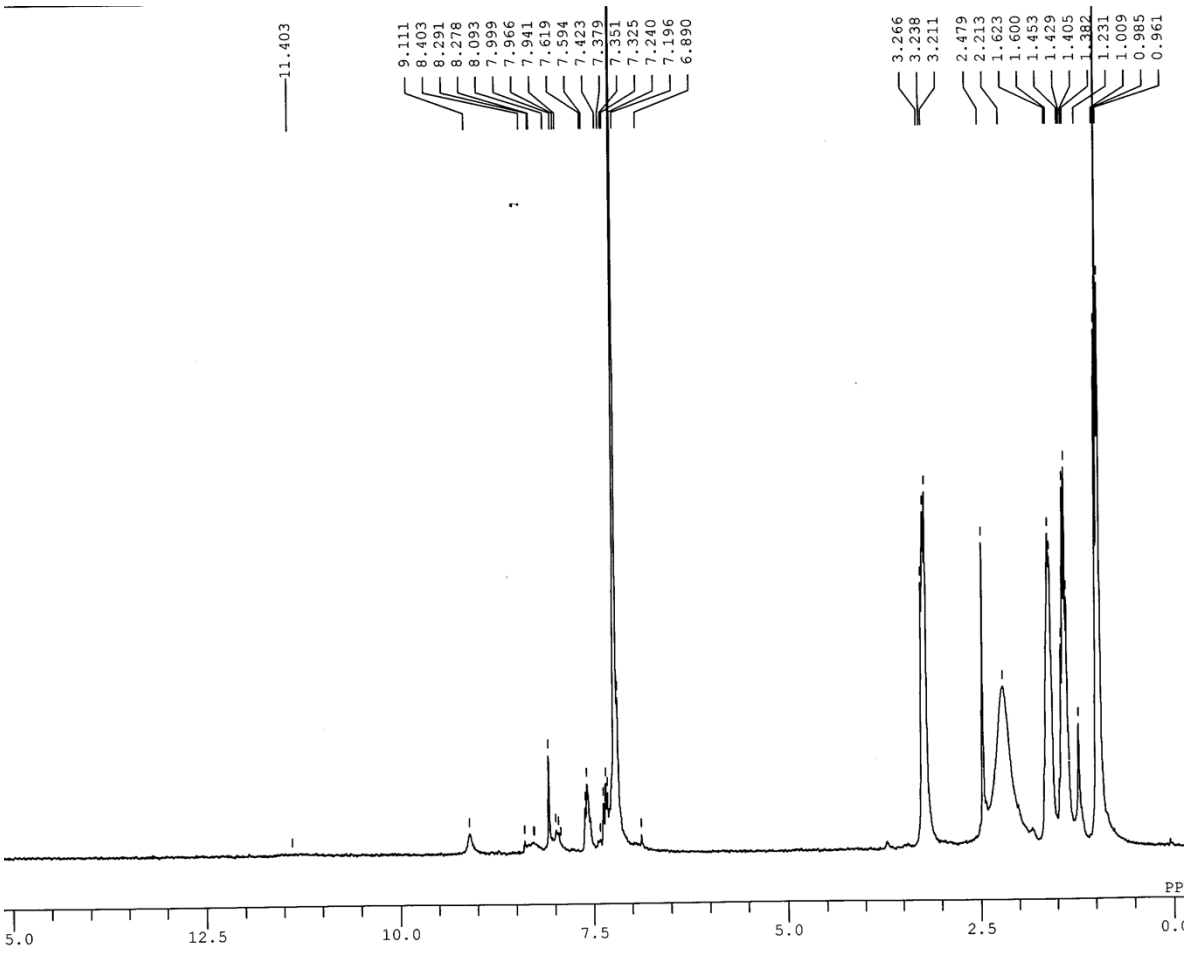

Figure S19: ^{1}H NMR titration spectrum of **3** with 0.6 equiv of F^- in $CDCl_3$.

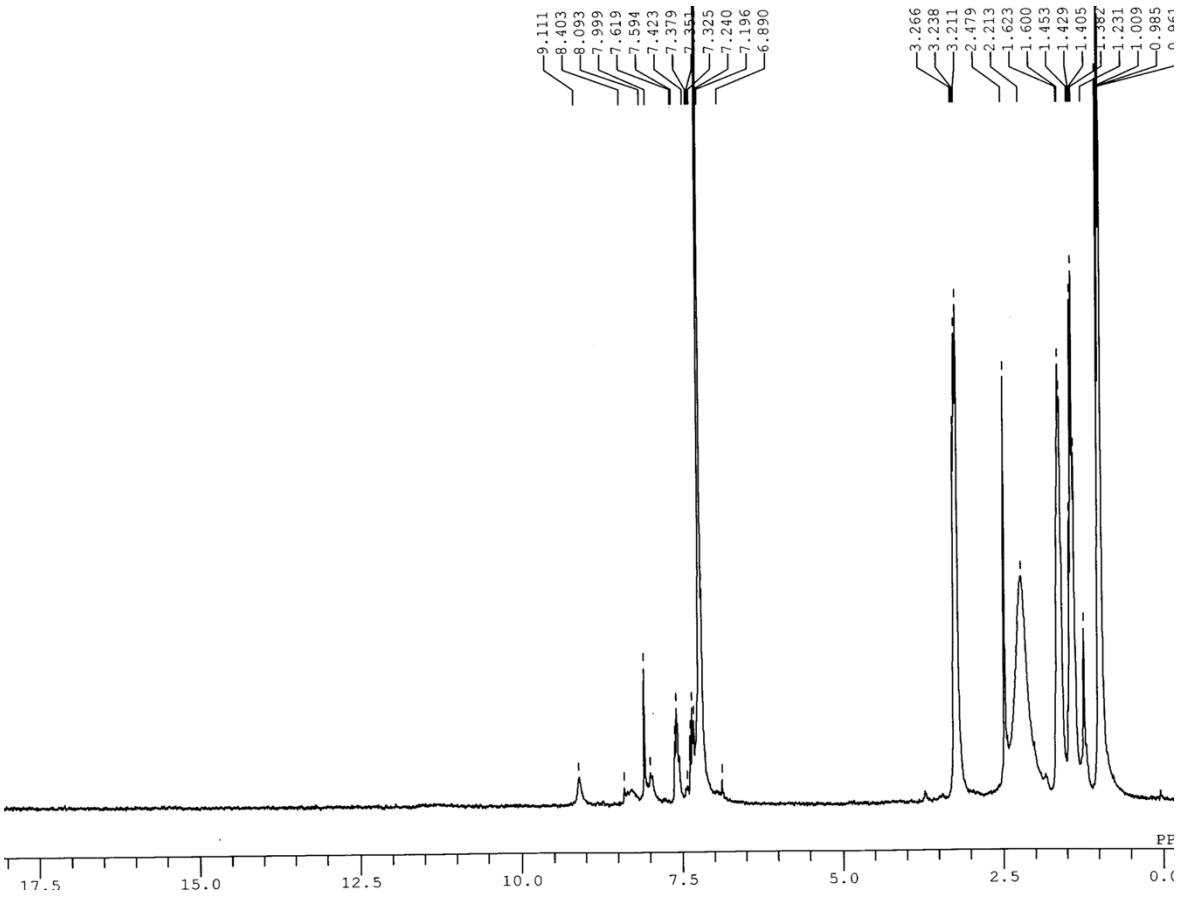

Figure S20: ^{1}H NMR titration spectrum of **3** with 0.8 equiv of F^- in $CDCl_3$.

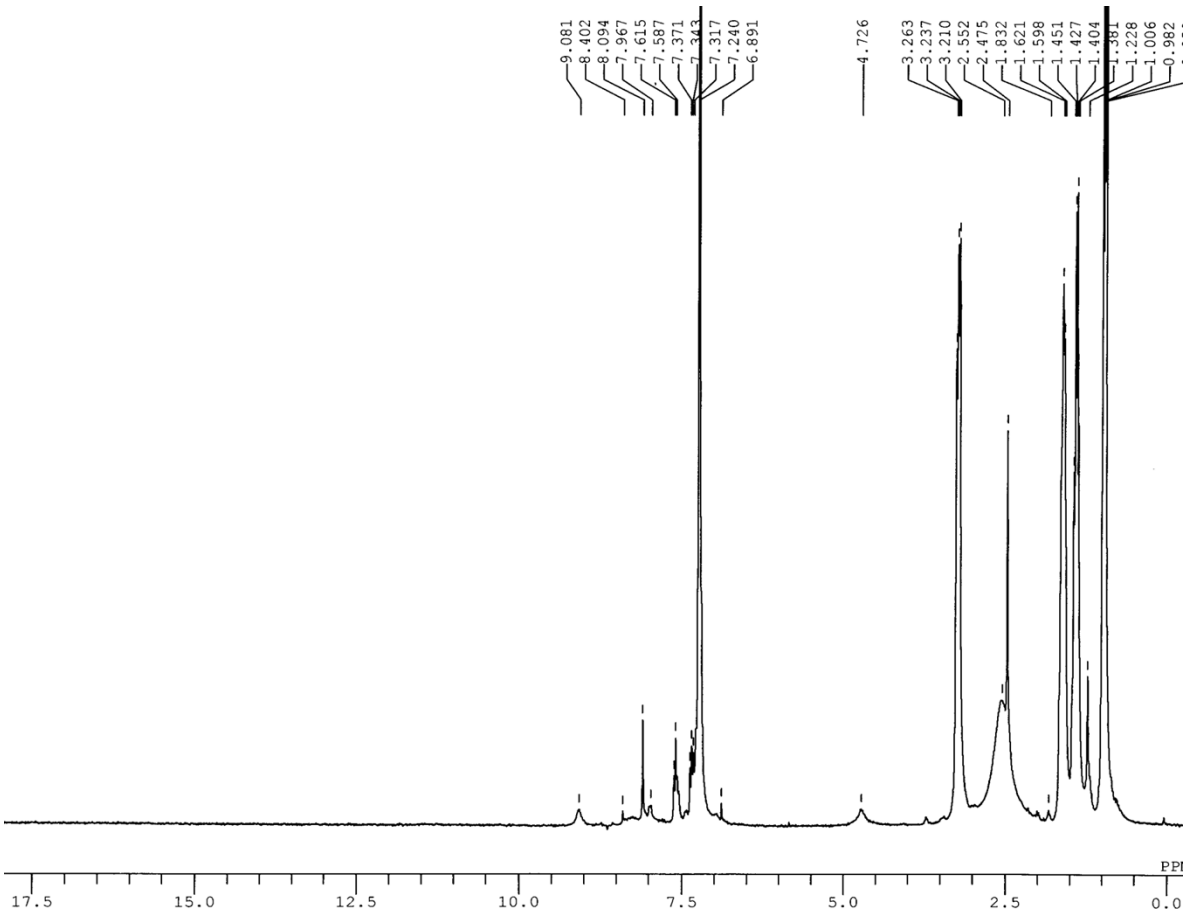

Figure S21: ^{1}H NMR titration spectrum of **3** with 1.2 equiv of F^- in $CDCl_3$.

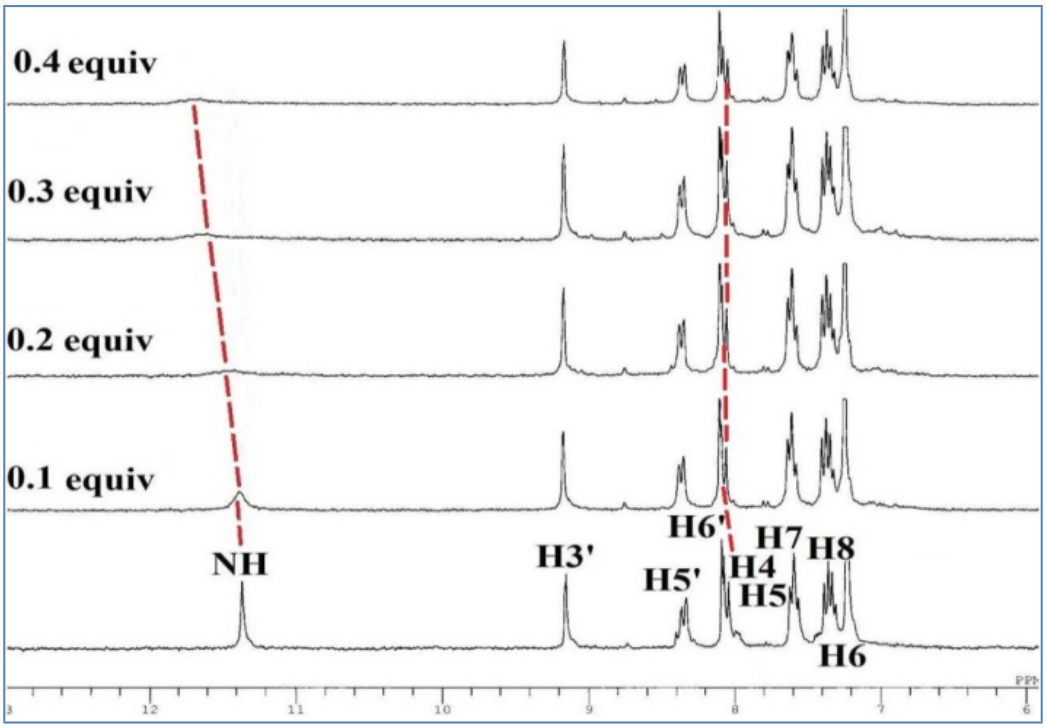

Figure S22: Stacked ^{1}H NMR titration spectra of **3** upon addition of AcO^{-} (0, 0.1, 0.2, 0.3, and 0.4 equiv) in $CDCl_3$.

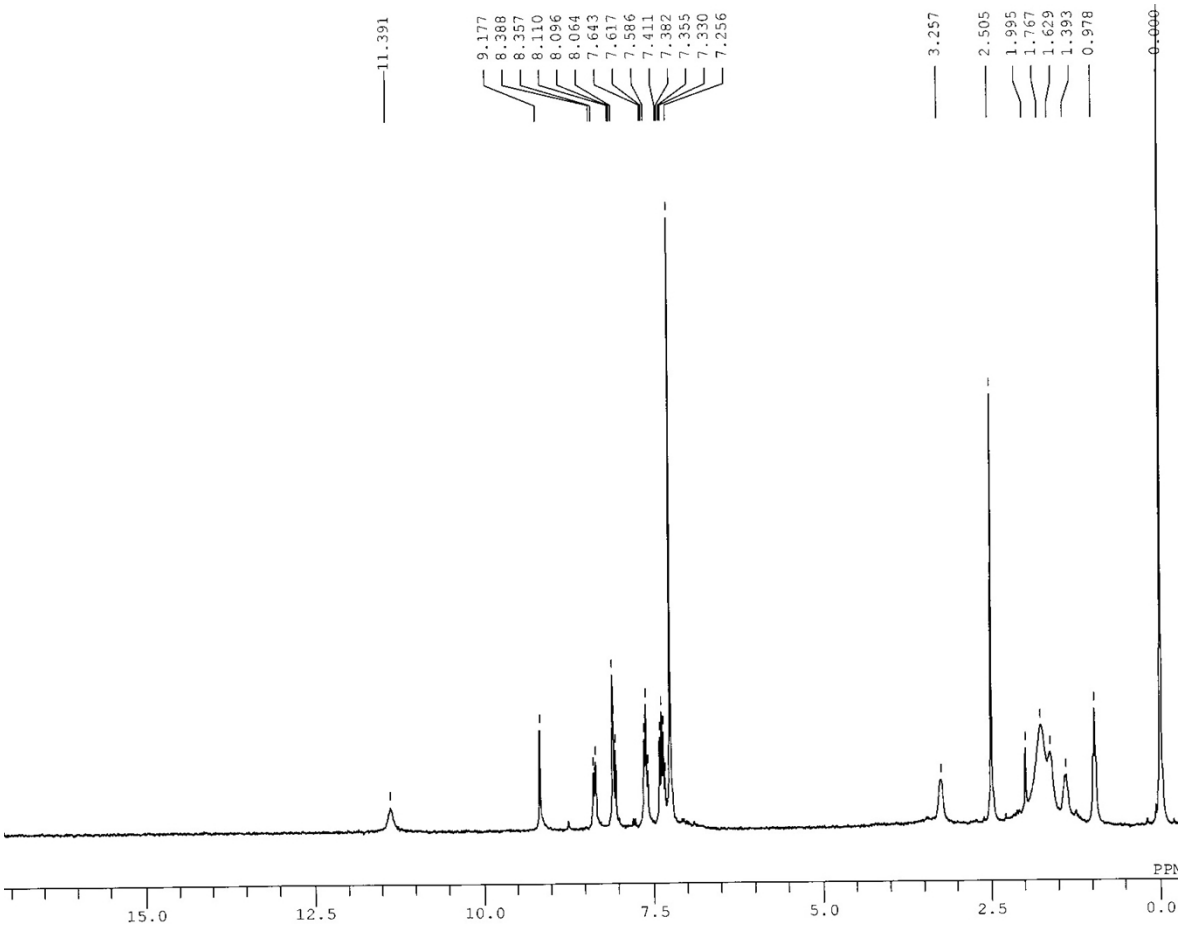

Figure S23: ^{1}H NMR titration spectrum of **3** with 0.1 equiv of AcO^{-} in $CDCl_3$.

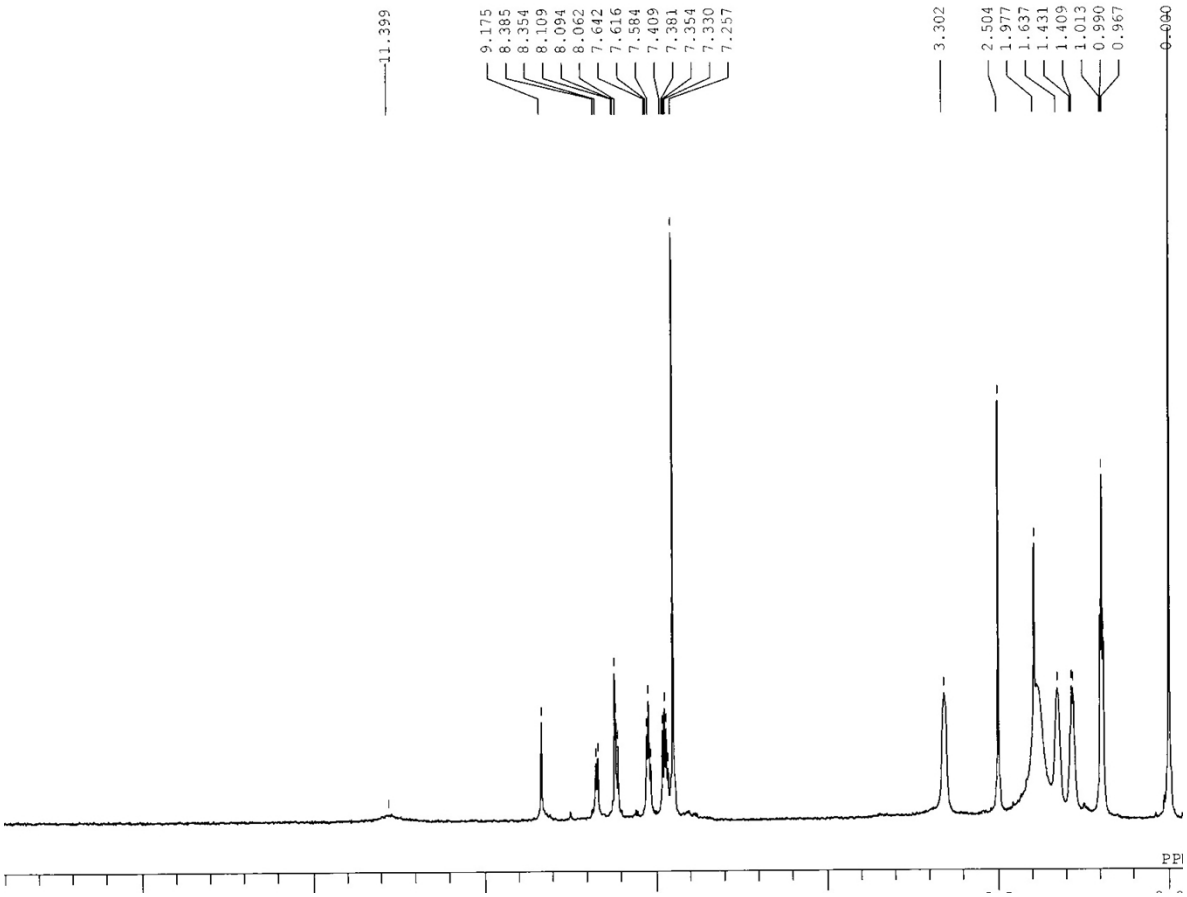

Figure S24: ^{1}H NMR titration spectrum of **3** with 0.2 equiv of AcO^{-} in $CDCl_3$.

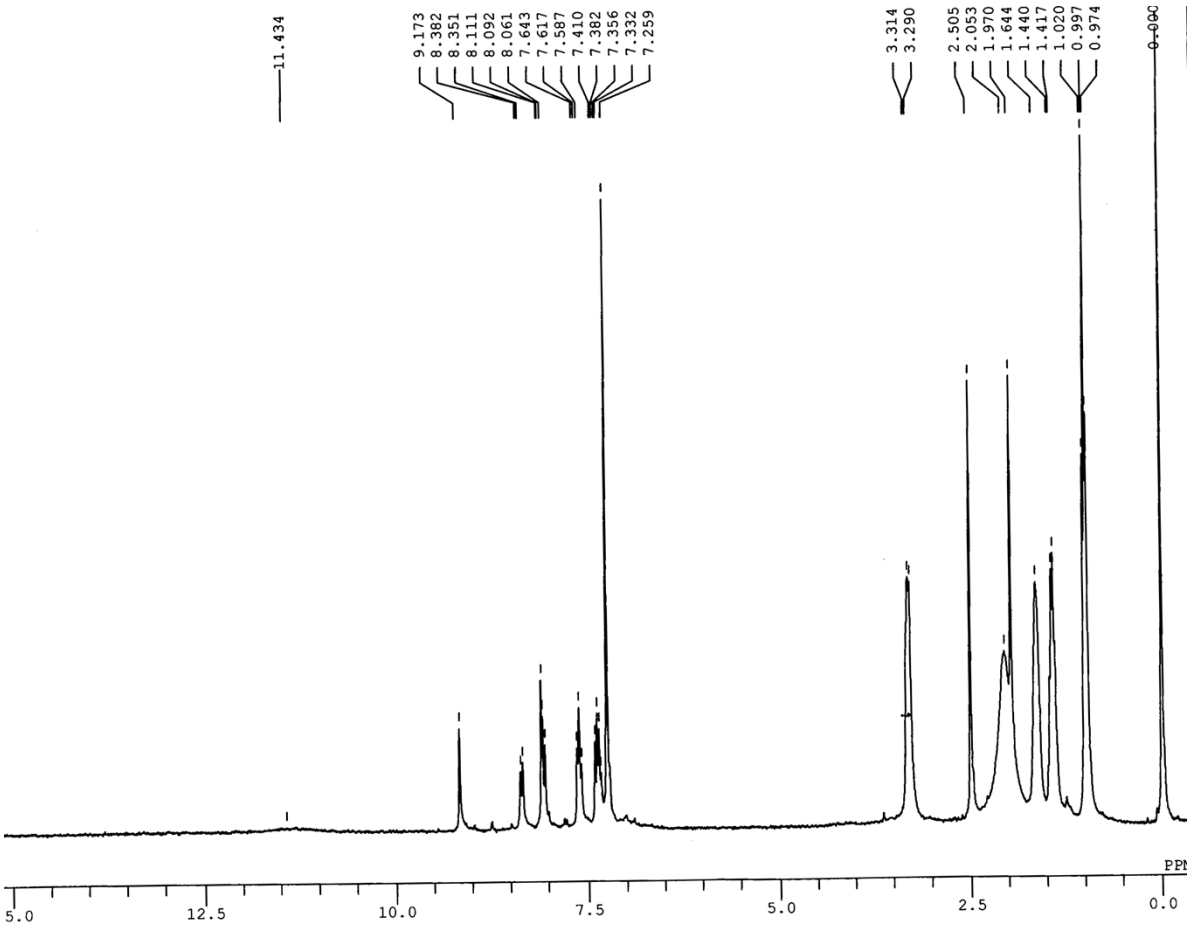

Figure S25: ^{1}H NMR titration spectrum of **3** with 0.3 equiv of AcO^{-} in $CDCl_3$.

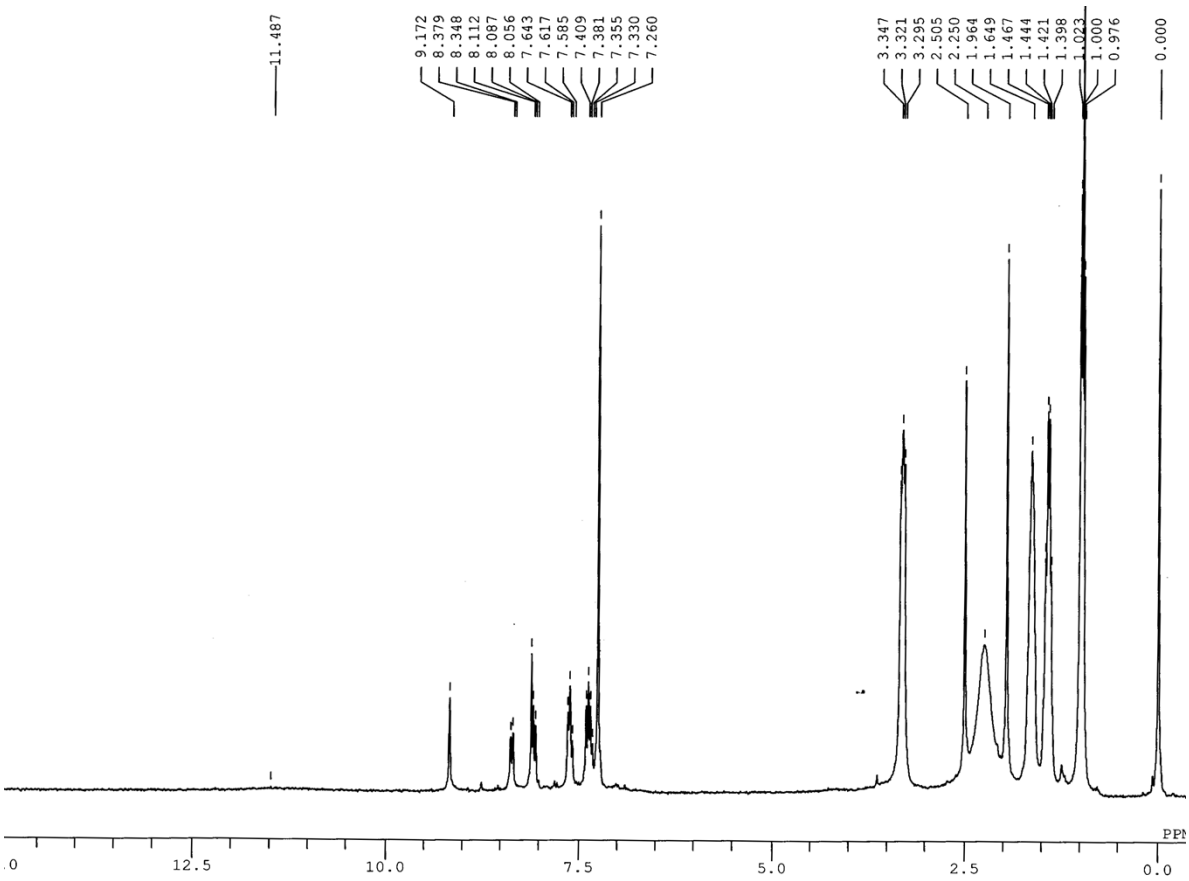

Figure S26: ^{1}H NMR titration spectrum of **3** with 0.4 equiv of AcO^{-} in $CDCl_3$.

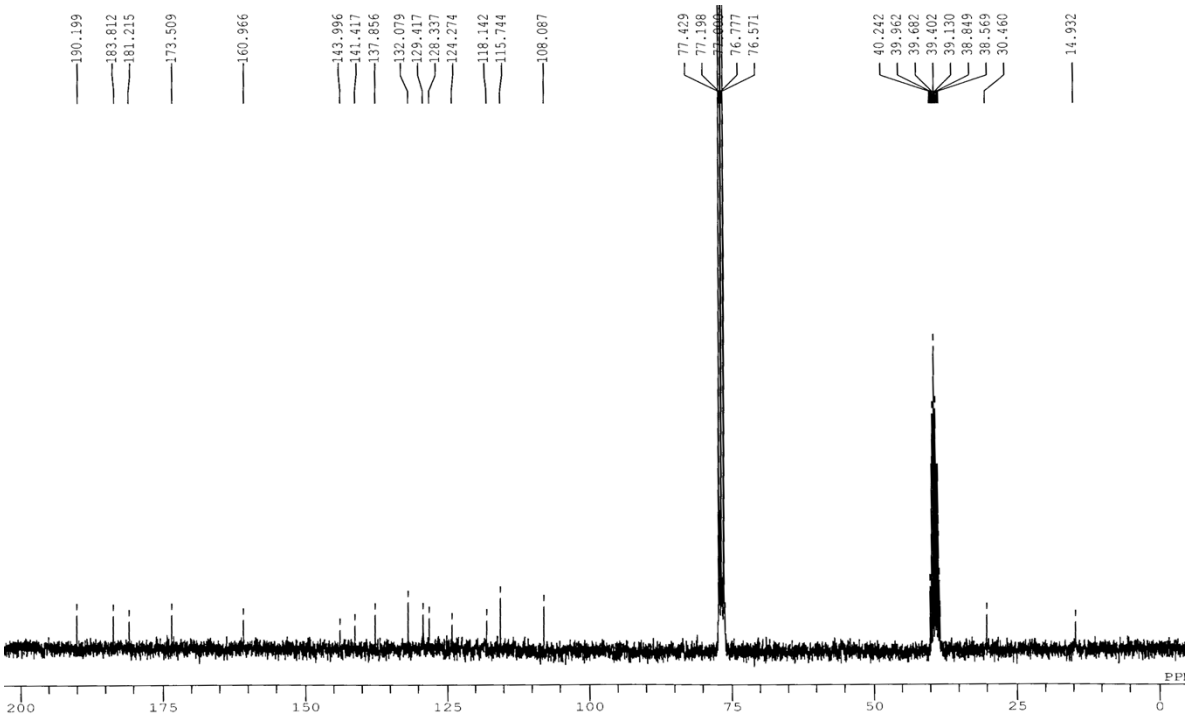

Figure S27: ^{13}CNMR spectrum of adduct, **3-CN**$^{-}$ in $CDCl_3$/DMSO-d_6.

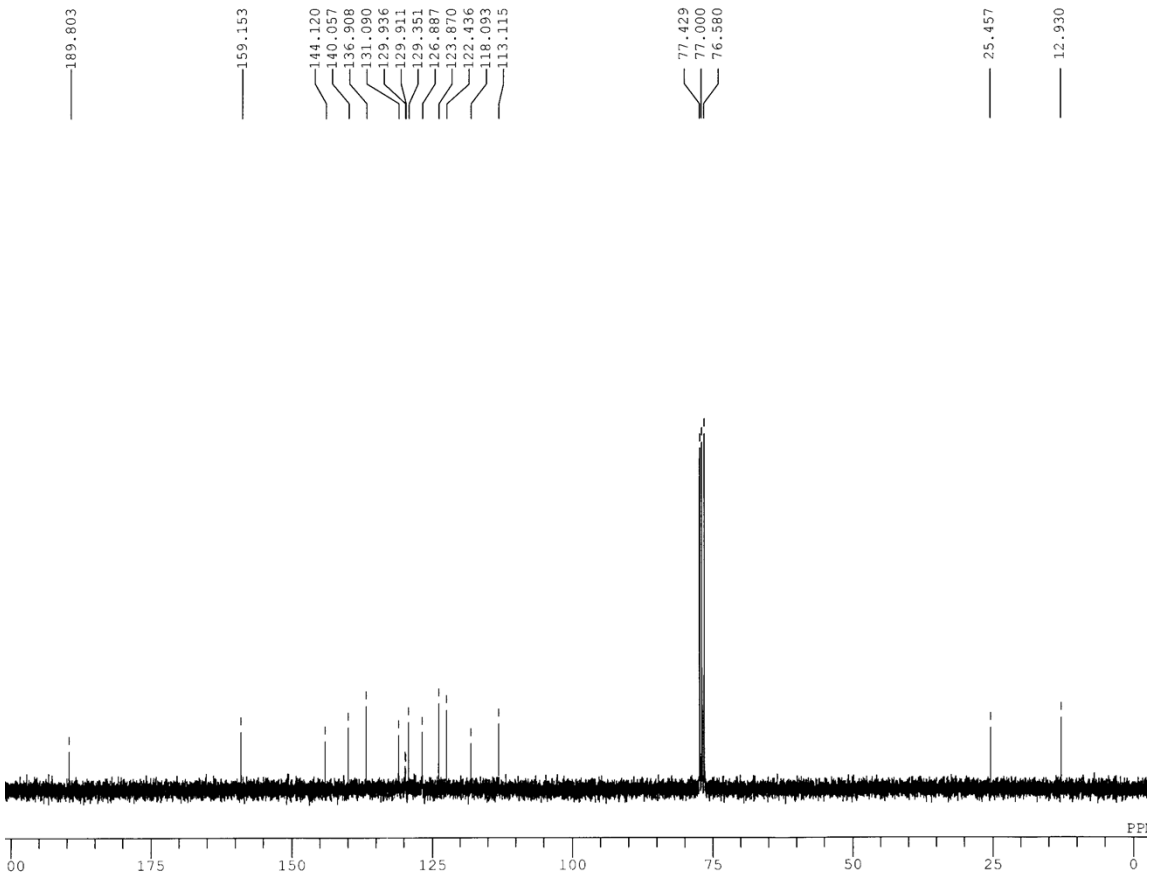

Figure S28: ^{13}CNMR spectrum of adduct, **4-CN**$^{-}$ in $CDCl_3$.

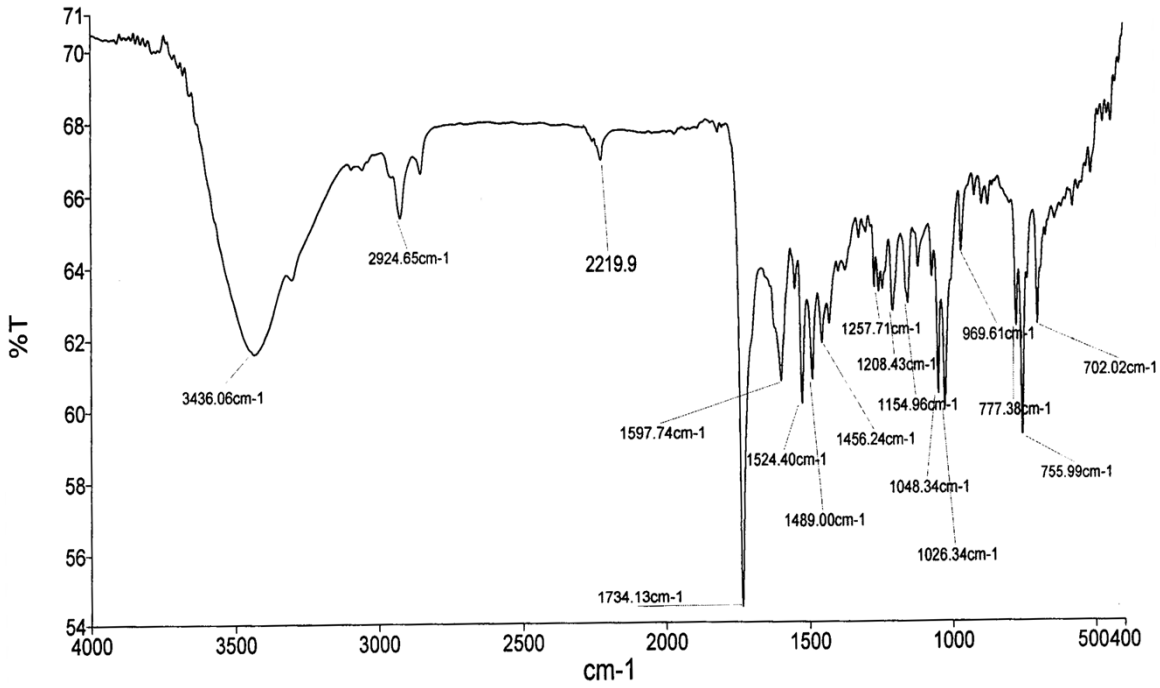

Figure S29: FTIR spectrum of adduct, **3-CN**$^{-}$.

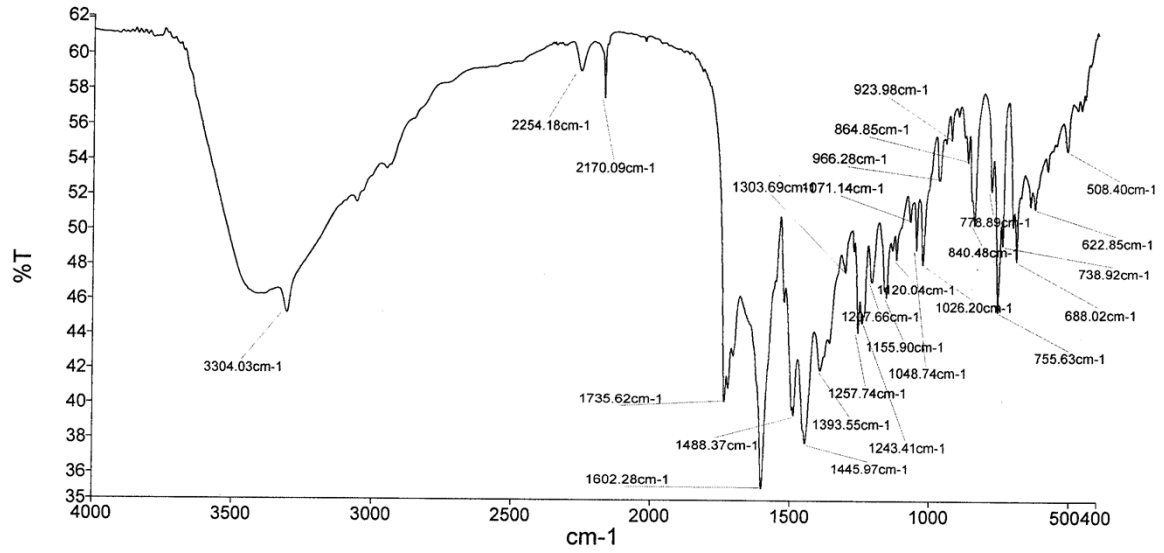

Figure S30: FTIR spectrum of adduct, **4-CN**$^{-}$.

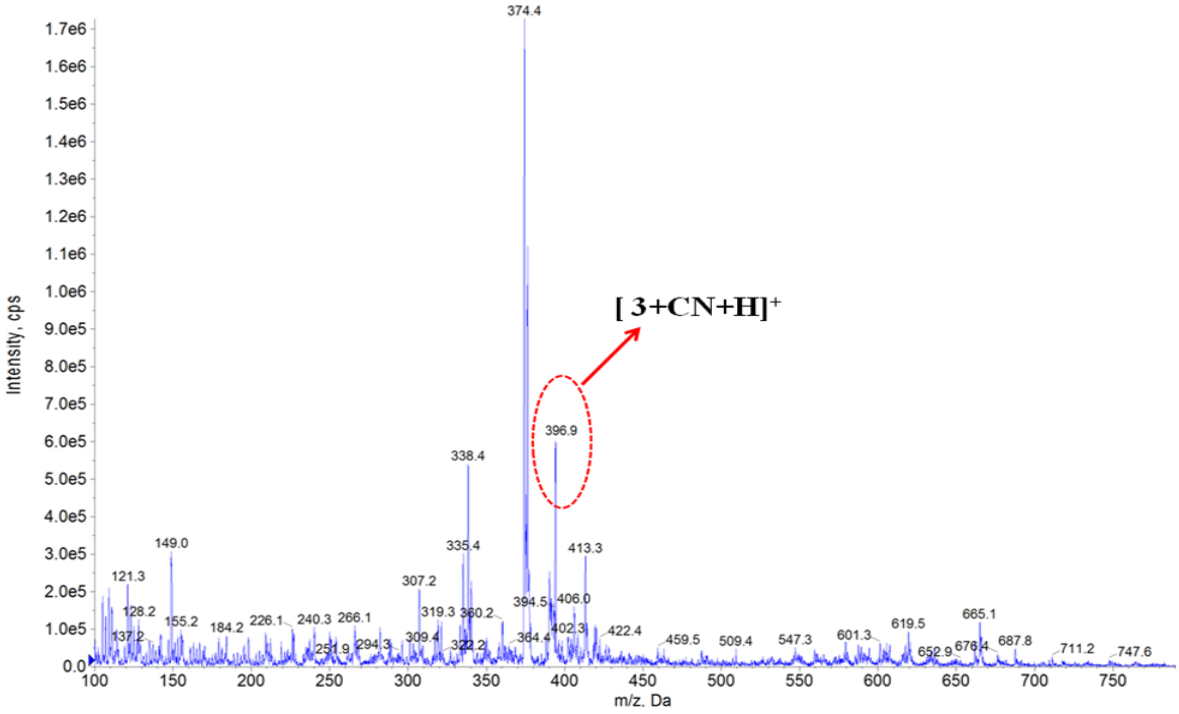

Figure S31: Mass spectrum (ESI-MS) of **3-CN**.

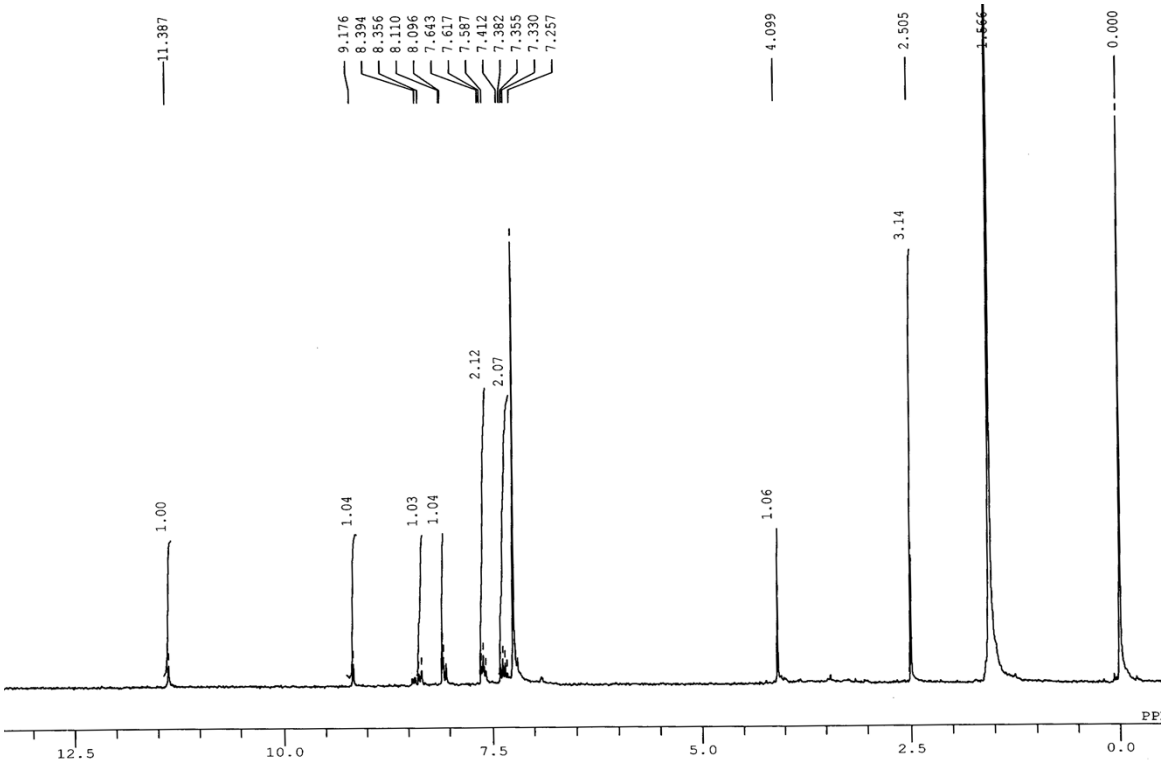

Figure S32: ^{1}HNMR spectrum of adduct, **3-CN**$^{-}$.

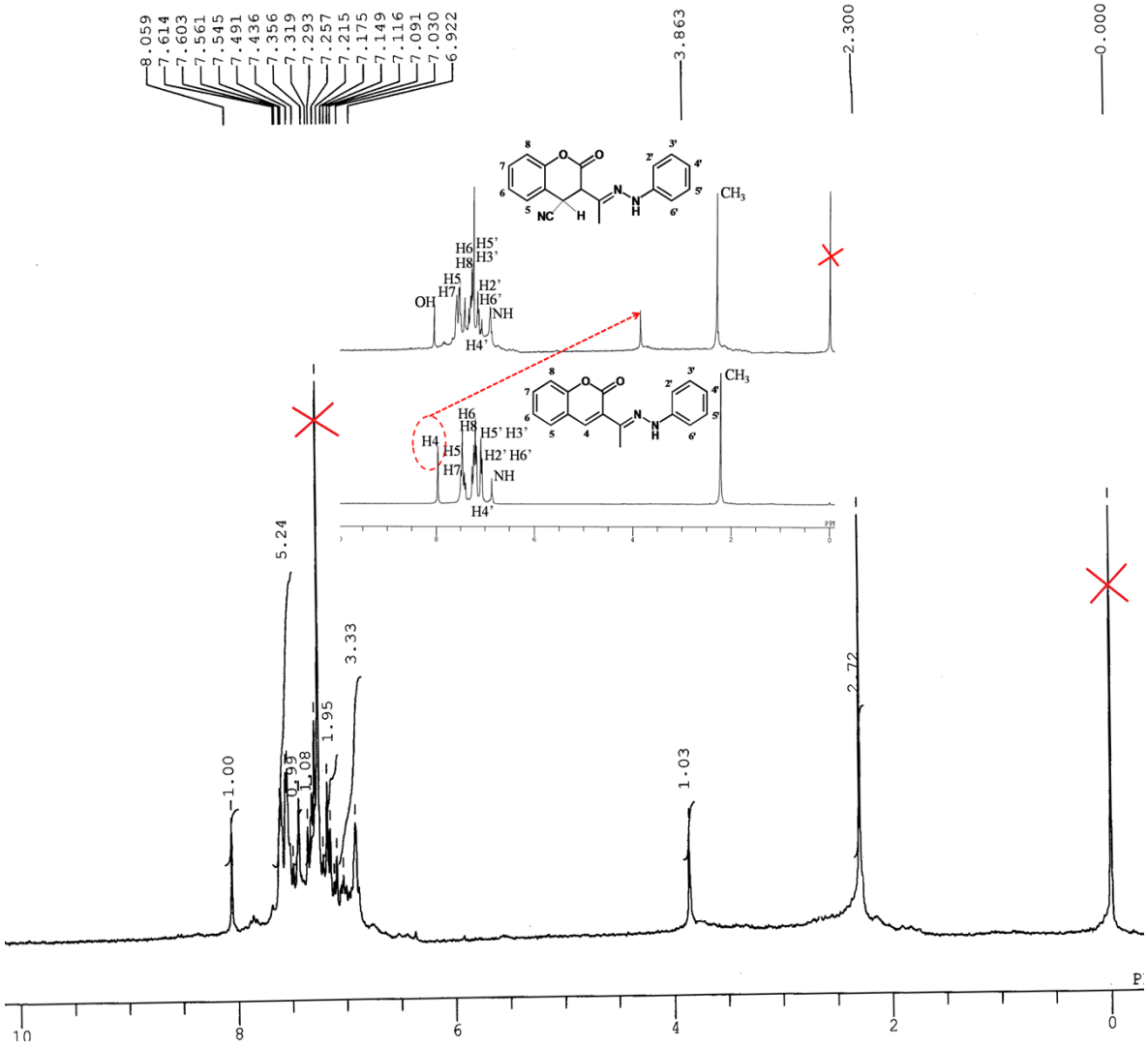

Figure S33: [1]HNMR spectrum of adduct, **4-CN**$^{-}$. Inset: stacked [1]H-NMR spectra of **4** and **4-CN**$^{-}$.

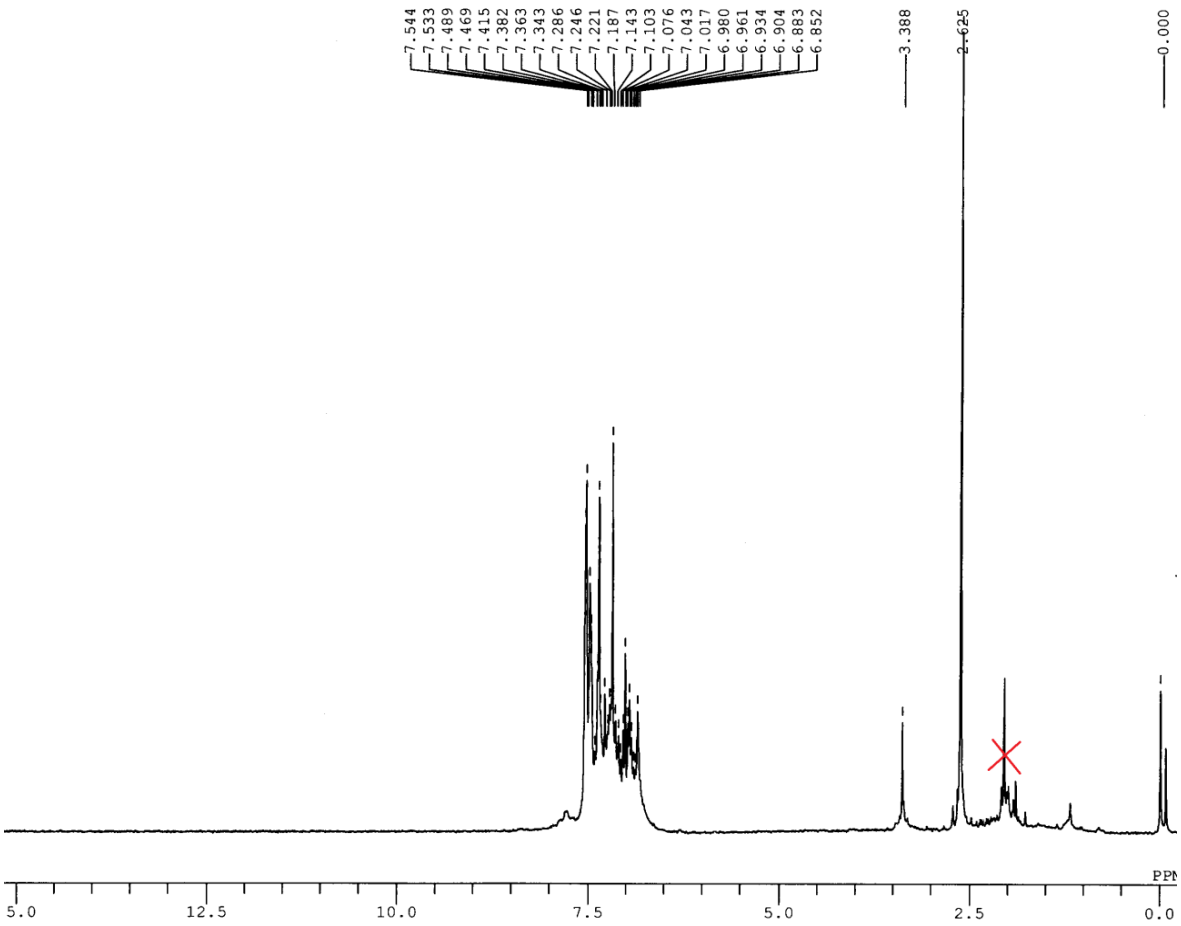

Figure S34: D_2O exchange ^{1}HNMR spectrum of adduct, **4-CN$^-$**.

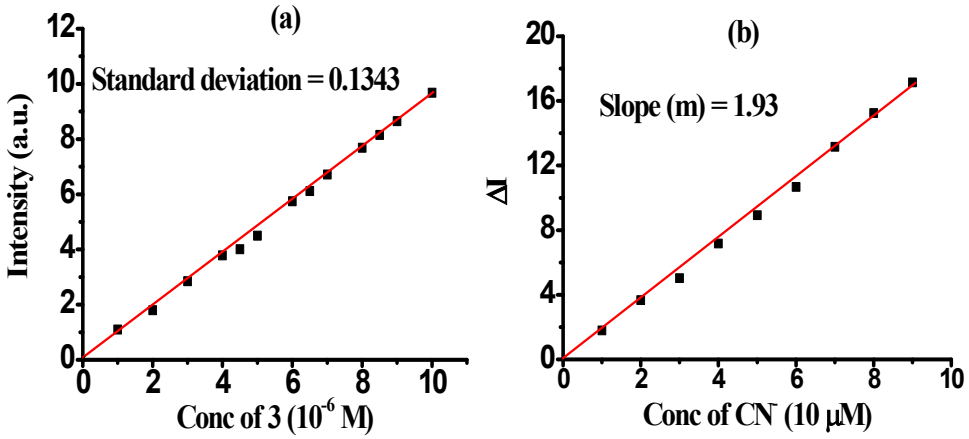

Figure S35: (a) Calibration curve for **3,** (b) calibration sensitivity for CN^- in H_2O.

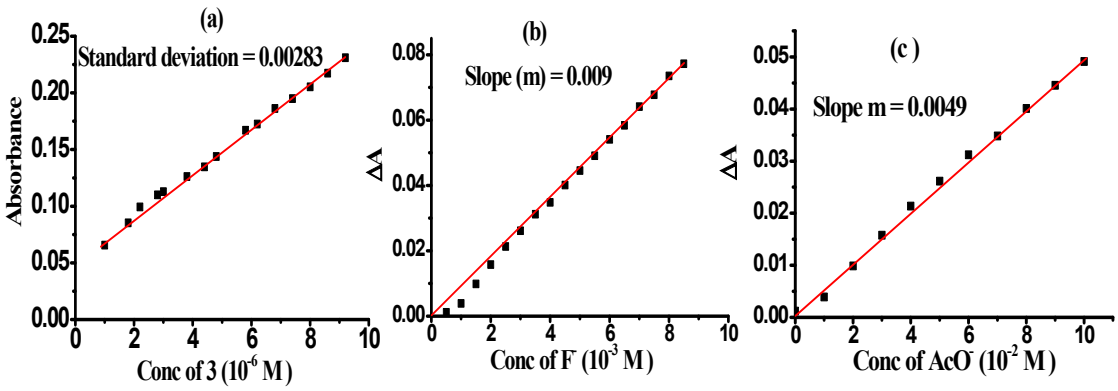

Figure S36: (a) Calibration curve for **3,** (b) and (c) calibration sensitivities for F^- and AcO^- in MeCN.

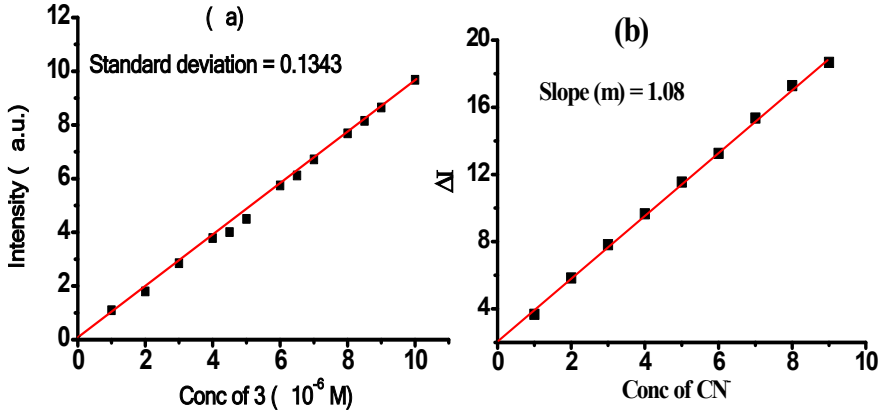

Figure S37: (a) Calibration curve for **3,** (b) calibration sensitivity for CN^- in human blood plasma.

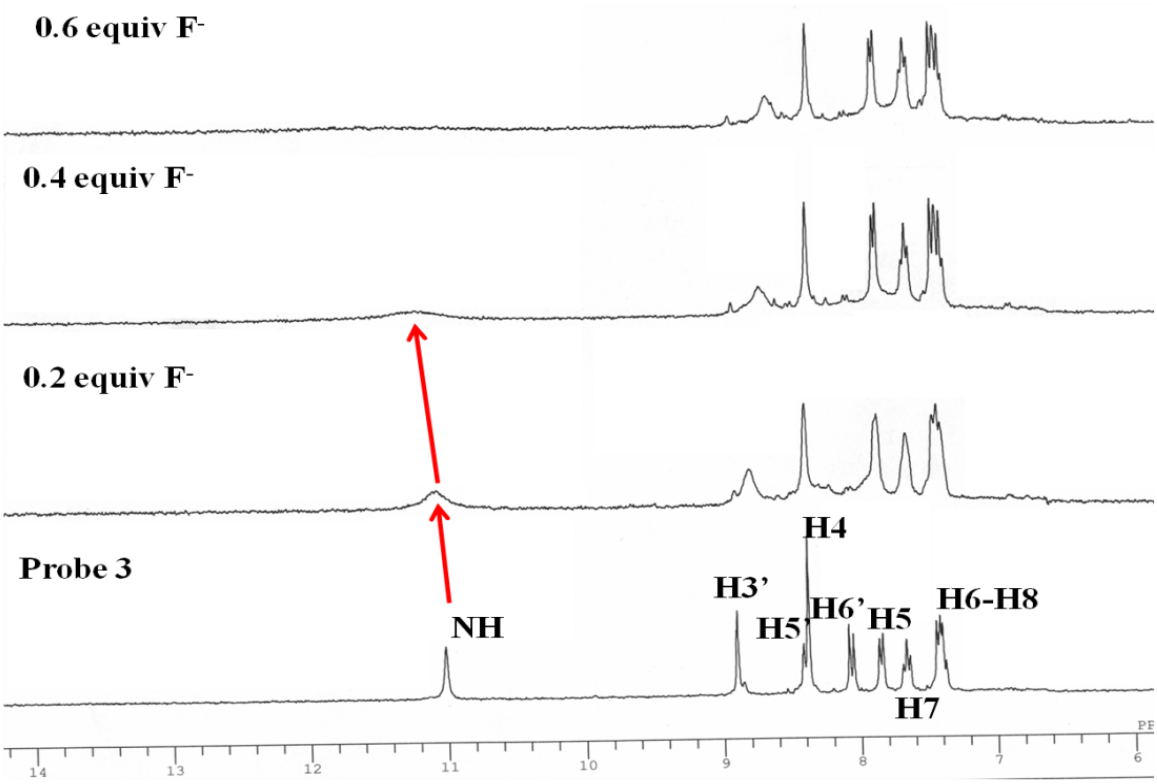

Figure S38: Stacked ^{1}H NMR titration spectra of **3** upon addition of F^- (0, 0.2, 0.4 and 0.6 equiv) in DMSO.

Further, to prove the H-bonding or deprotonation, ^{1}H NMR titration studies has been performed in DMSO-d_6 ($c = 2 \times 10^{-1}$ mol l^{-1}). In ^{1}H NMR spectrum of **3** (Figure S38) singlet appeared at δ 11.017, 8.907 and 8.381 ppm are attributable to resonances of -*N*H, H3' and H4 protons while resonances at δ 8.423 (d, J = 2.4 Hz), 8.086 (d, J = 9.3 Hz), 7.866 (d, J = 7.8 Hz), 7.692 (t, J_1 = 7.5, J_2 = 8.1 Hz), 7.444-7.376 (m) ppm are assignable to H5', H6', H5, H7, and H6 H8 protons respectively. Upon addition of 0.2 equiv. of F^- to a solution of **3, -*NH*** signal shifted toward downfield and appeared at 11.066 ppm (Figure S39) whereas H3', H6', H7 protons shifted upfield and H4, H5, H6-H8 protons shifted slightly downfield. However, upon increasing the concentration of F^- ions (0.4 equiv.) the -*N*H signal shifted downfield to appear at δ 11.232 (Δδ =0.215) ppm while H3', H6', H7, H4 protons shifted upfield and H5, H6-H8 protons signal was shifted downfield to appear at δ 8.702, 8.084, 7.663, 8.354 and 7.871 and 7.445 ppm respectively (Figure S40) whereas H5' signal merged in H4. Further, increasing the concentration of F^- (0.6 equiv) to a solution of **3**,-*NH* signal broadened and disappeared while H4 shifted toward upfield, δ = 8.329 (Δδ = 0.052) ppm and all the ring protons shifted upfield region (Figure S41). Thus, suggested about the possibility of H-bonding interaction between **3** and F^- involving H4 and –*N*H protons.

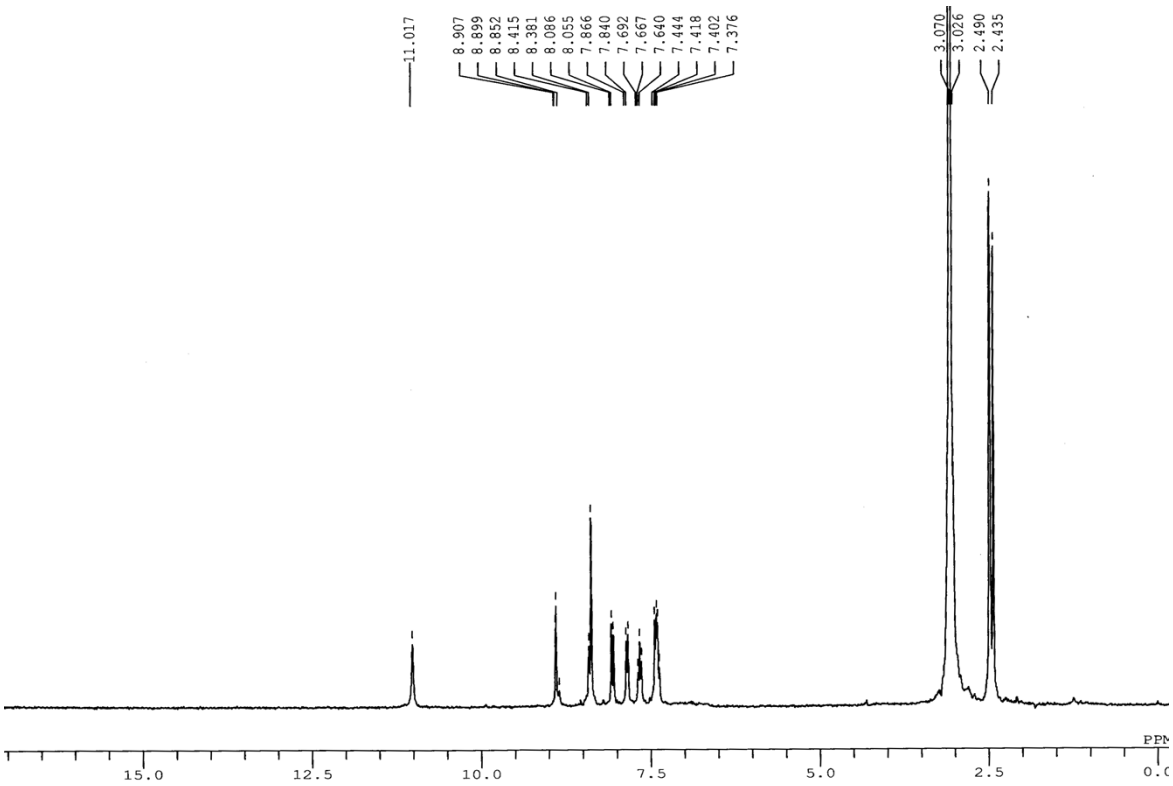

Figure S39: ^{1}H NMR spectrum of **3** in DMSO-d_6.

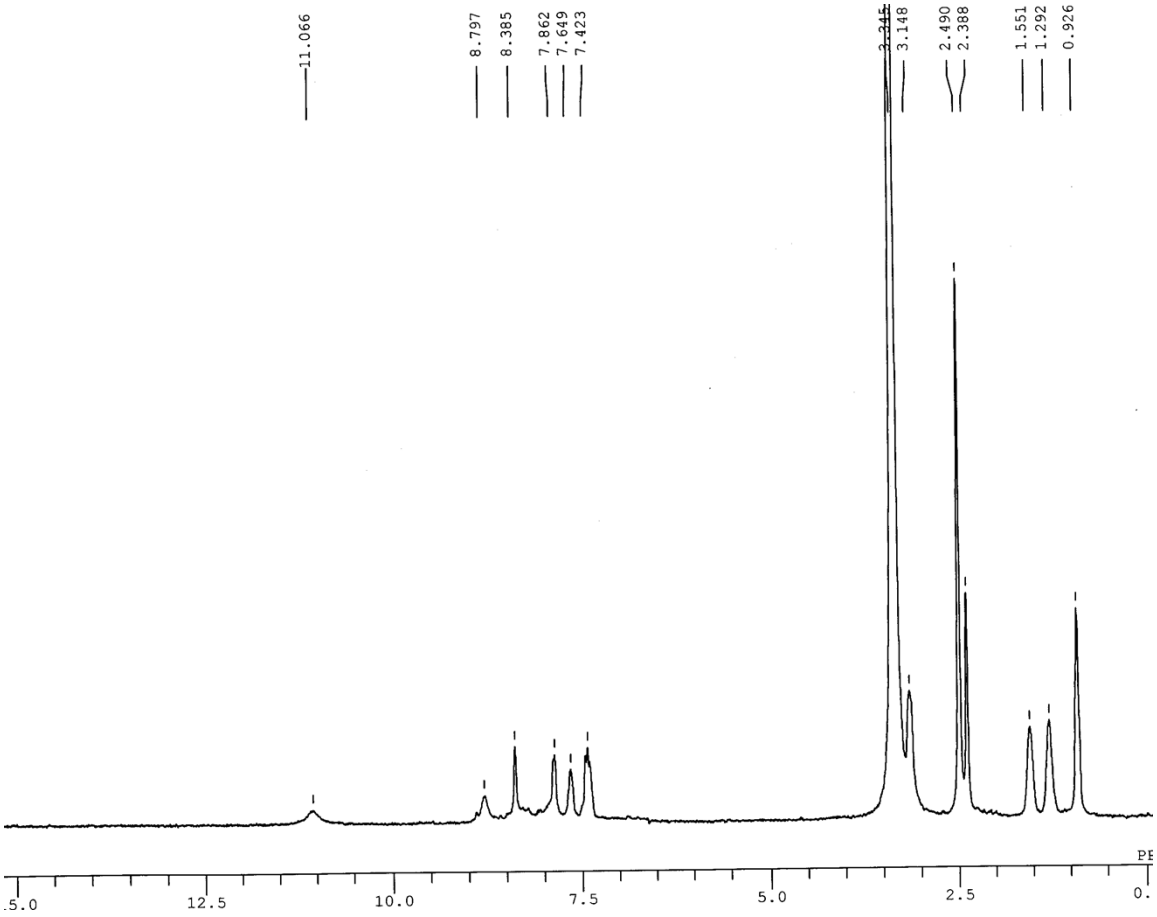

Figure S40: ^{1}H NMR titration spectrum of **3** with 0.2 equiv of F^- in DMSO-d_6.

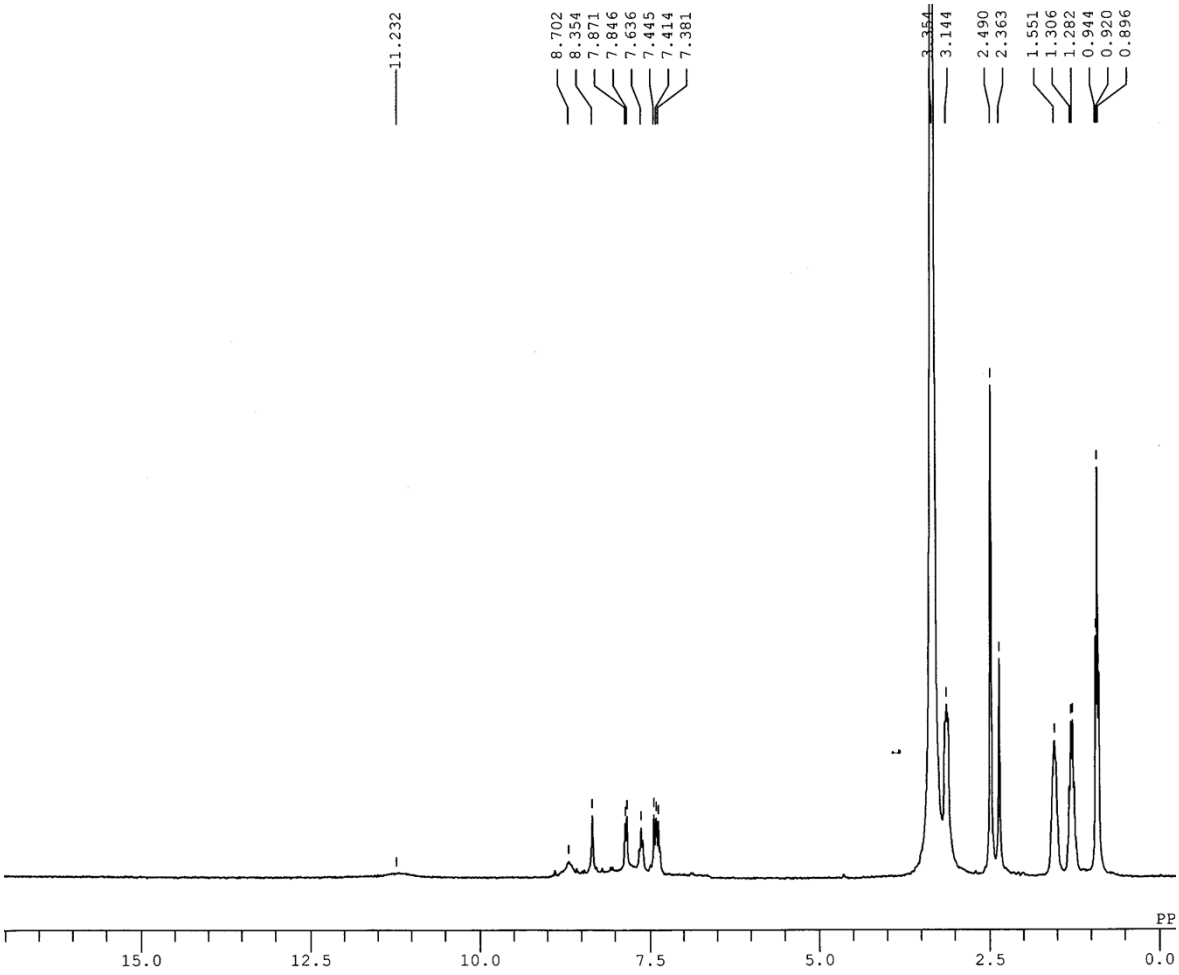

Figure S41: ^{1}H NMR titration spectrum of **3** with 0.4 equiv of F^- in DMSO-d_6.

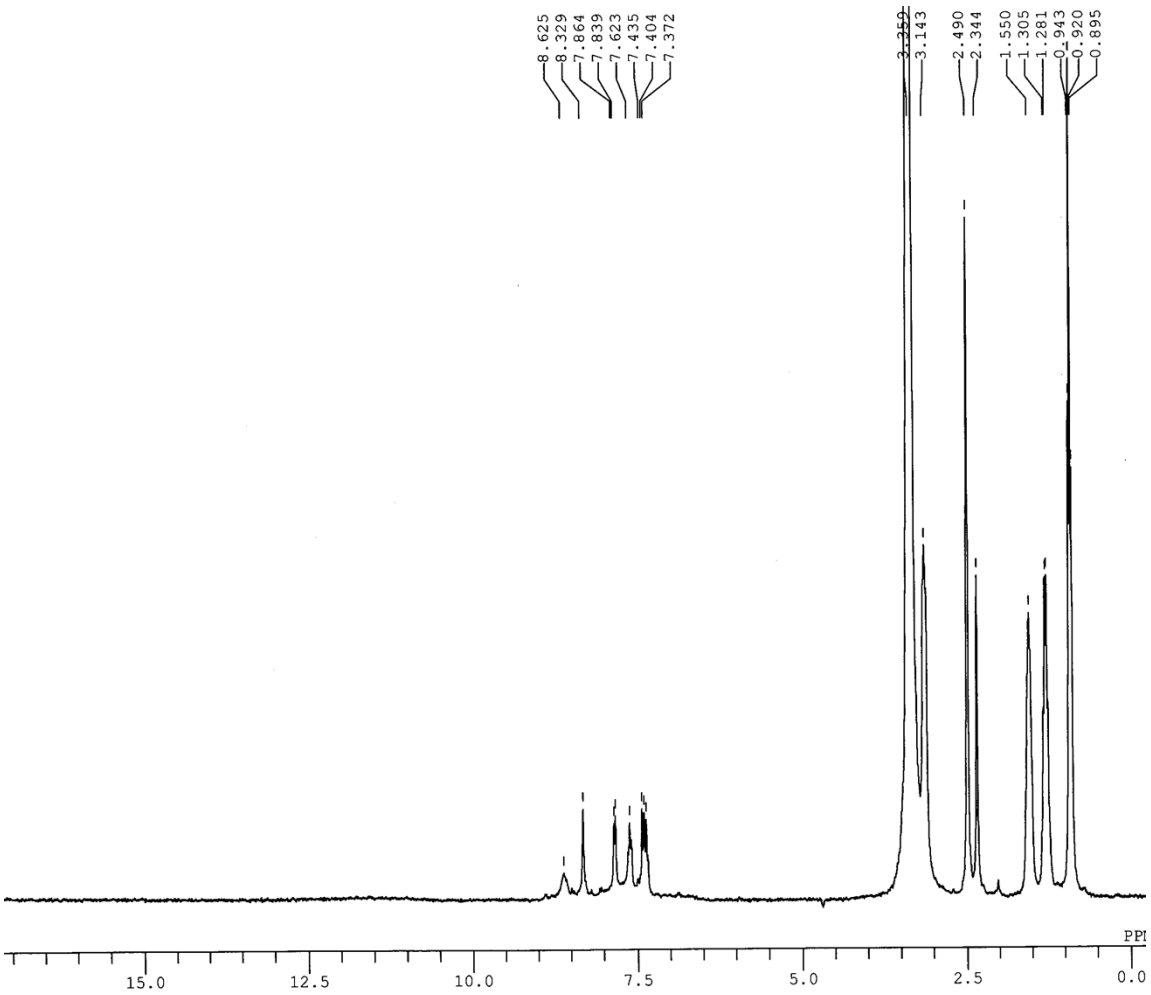

Figure S42: ^{1}H NMR titration spectrum of **3** with 0.6 equiv of F^- in DMSO-d_6.